NASA/TP—2009–215634

Developing a Material Strength Design Value Based on Compression After Impact Damage for the Ares I Composite Interstage

A.T. Nettles and J.R. Jackson
Marshall Space Flight Center, Marshall Space Flight Center, Alabama

January 2009

The NASA STI Program…in Profile

Since its founding, NASA has been dedicated to the advancement of aeronautics and space science. The NASA Scientific and Technical Information (STI) Program Office plays a key part in helping NASA maintain this important role.

The NASA STI program operates under the auspices of the Agency Chief Information Officer. It collects, organizes, provides for archiving, and disseminates NASA's STI. The NASA STI program provides access to the NASA Aeronautics and Space Database and its public interface, the NASA Technical Report Server, thus providing one of the largest collections of aeronautical and space science STI in the world. Results are published in both non-NASA channels and by NASA in the NASA STI Report Series, which includes the following report types:

- TECHNICAL PUBLICATION. Reports of completed research or a major significant phase of research that present the results of NASA programs and include extensive data or theoretical analysis. Includes compilations of significant scientific and technical data and information deemed to be of continuing reference value. NASA's counterpart of peer-reviewed formal professional papers but has less stringent limitations on manuscript length and extent of graphic presentations.

- TECHNICAL MEMORANDUM. Scientific and technical findings that are preliminary or of specialized interest, e.g., quick release reports, working papers, and bibliographies that contain minimal annotation. Does not contain extensive analysis.

- CONTRACTOR REPORT. Scientific and technical findings by NASA-sponsored contractors and grantees.

- CONFERENCE PUBLICATION. Collected papers from scientific and technical conferences, symposia, seminars, or other meetings sponsored or cosponsored by NASA.

- SPECIAL PUBLICATION. Scientific, technical, or historical information from NASA programs, projects, and missions, often concerned with subjects having substantial public interest.

- TECHNICAL TRANSLATION. English-language translations of foreign scientific and technical material pertinent to NASA's mission.

Specialized services also include creating custom thesauri, building customized databases, and organizing and publishing research results.

For more information about the NASA STI program, see the following:

- Access the NASA STI program home page at <http://www.sti.nasa.gov>

- E-mail your question via the Internet to <help@sti.nasa.gov>

- Fax your question to the NASA STI Help Desk at 443–757–5803

- Phone the NASA STI Help Desk at 443–757–5802

- Write to:
  NASA STI Help Desk
  NASA Center for AeroSpace Information
  7115 Standard Drive
  Hanover, MD 21076–1320

NASA/TP—2009–215634

Developing a Material Strength Design Value Based on Compression After Impact Damage for the Ares I Composite Interstage

A.T. Nettles and J.R. Jackson
Marshall Space Flight Center, Marshall Space Flight Center, Alabama

National Aeronautics and
Space Administration

Marshall Space Flight Center • MSFC, Alabama 35812

January 2009

TRADEMARKS

Trade names and trademarks are used in this report for identification only. This usage does not constitute an official endorsement, either expressed or implied, by the National Aeronautics and Space Administration.

Available from:

NASA Center for AeroSpace Information
7115 Standard Drive
Hanover, MD 21076–1320
443–757–5802

This report is also available in electronic form at
<https://www2.sti.nasa.gov>

TABLE OF CONTENTS

1. INTRODUCTION 1

2. MATERIALS 3

3. TESTING 4

3.1 Boundary Condition Selection 4
3.2 Impact Testing 6
3.3 Environmental Effects 8
3.4 Residual Strength Testing 11

4. RESULTS 16

4.1 Damage Detection Threshold 16
4.2 Impact of Specimens to be Compression Tested 21
4.3 Environmental Effects 23
4.4 Compression After Impact Residual Strength Versus Damage Size 24
4.5 Compression After Impact Versus Dent Depth 31

5. CALCULATING A MATERIAL STRENGTH DESIGN VALUE 35

6. CONCLUSIONS 36

REFERENCES 37

LIST OF FIGURES

1. Schematic of the three boundary conditions used in the first series of impacts: (a) flex, (b) loose, and (c) solid 5

2. The NDE size versus impact energy results of the boundary condition tests 5

3. Schematic of impact test apparatus 6

4. Schematic of impact test specimen with impact locations 7

5. Flash thermography images of two 16-ply face sheet specimens impacted at 5.0 ft lb with (a) 0.25- and (b) 0.5-in tups 8

6. Flash thermography of a 16-ply face sheet specimen impacted at 7.5 ft lb with a 1.5-in tup 8

7. Open hole compression specimens used for environmental effects study 9

8. Moisture gain for first batch of specimens 10

9. Moisture gain for second batch of specimens 10

10. Photograph of a CAI specimen prior to compression testing (a) front view and (b) bottom view 12

11. Schematic of a CAI test specimen: (a) front view and (b) bottom view 12

12. (a) A buckled and (b) end broomed specimen 13

13. Specimen in a load frame 13

14. Typical load versus strain plot for 16-ply CAI specimens 14

15. Typical load versus strain plot for 18-ply specimens 15

16. Non-destructive evaluation detection size versus impact energy for 16- and 18-ply facesheet specimens impacted with a 0.25-in tup 16

17. Non-destructive detection size versus impact energy for 16-ply facesheet specimens impacted with a 0.5-in tup 17

LIST OF FIGURES (Continued)

18. Non-destructive detection size versus impact energy for 16- and 18-ply facesheet specimens impacted with a 1.5-in tup 17

19. Ultraviolet light enhanced photomicrograph of specimen 16-10-5. No damage detected by flash thermography. Minor delaminations and microcracking about one-half-cell width in size 19

20. Ultraviolet light enhanced photomicrograph of specimen 16-10-5. No damage detected by flash thermography. Minor damage less than one-cell width seen 19

21. Ultraviolet light enhanced photomicrograph of specimen 16-10-4. Damage size of 0.625 in detected by flash thermography. Delaminations are clearly visible 20

22. Ultraviolet light enhanced photomicrograph of specimen 18-9. No damage detected by flash thermography. No damage seen upon cross-sectioning 20

23. Ultraviolet light enhanced photomicrograph of specimen 18-5. Flash thermography showed an indication size of 0.585 20

24. Open hole compression testing results of the various dwell times at 220 ºF 23

25. Compression after impact results for various temperatures at a 10-min dwell time ... 24

26. Failed 16-ply compression after impact specimen : (a) front view and (b) side view ... 24

27. Failed 18-ply compression after impact specimen: (a) front view and (b) side view 25

28. Residual strength versus damage size for all 16-ply impacted specimens 25

29. Power curve fit to strength degradation portion of residual strength curve for 16-ply specimens 26

30. B-basis CAI curve plotted with experimental data for the 16-ply specimens 28

31. Residual strength versus damage size for all 18-ply impacted specimens 28

32. Power curve fit to strength degradation portion of residual strength curve for the 18-ply specimens 29

33. B-basis CAI curve plotted with experimental data for the 18-ply specimens 30

34. Residual strength versus dent depth for all 18-ply impacted specimens 31

LIST OF FIGURES (Continued)

35. Power curve fit to strength degradation portion of dent depth residual strength curve for the 18-ply specimens 31

36. B-basis dent depth versus CAI curve plotted with experimental data for the 18-ply specimens 33

37. Damage size corresponding to A- and B-basis CAI curve for the 18-ply specimens 35

LIST OF TABLES

1. Summary of OHC specimens used to evaluate environmental effects 11

2. Summary of specimens that were cross-sectioned and examined microscopically 18

3. Summary of impacts on the 16-ply CAI samples 21

4. Summary of impacts on the 18-ply CAI samples 22

5. Residuals from data on the 16-ply specimens 27

6. Residuals from data on the 18-ply specimens 30

7. Residuals from dent depth data on the 18-ply specimens 32

LIST OF ACRONYMS AND SYMBOLS

ASTM	American Society for Testing and Materials
BDID	barely detectable impact damage
CAI	compression after impact
ECF	environmental correction factor
FAA	Federal Aviation Administration
IR	infrared
MSFC	Marshall Space Flight Center
NDE	non-destructive evaluation
OHC	open hole compression
OSL	observed significance level
RQMT	requirement
RT	room temperature
TP	technical publication

NOMENCLATURE

x	damage size in inches
$y(x)_B$	B-basis residual strength curve
$y(x)$	power curve fit, predicted CAI strength

TECHNICAL PUBLICATION

DEVELOPING A MATERIAL STRENGTH DESIGN VALUE BASED ON COMPRESSION AFTER IMPACT DAMAGE FOR THE ARES I COMPOSITE INTERSTAGE

1. INTRODUCTION

For a composite laminate to be used successfully in a structure, its damage tolerance capabilities must be understood. Impact damage can cause reductions in laminate strength (particularly compression) that must be accounted for during the life of the structure. How this is explained varies greatly with inspection methods, impact threats, redundant load paths (or lack thereof), and many other factors. While there is much literature, mostly analytical, involving impact damage to composite laminates, little information with experimental data on a significant number of test specimens can be found. This is mainly due to the highly proprietary nature of the data generated and the high cost involved in performing a damage tolerance program. A good example of publicly available data from a damage tolerance program is given in a series of reports from the Federal Aviation Administration (FAA).[1–4]

For next-generation manned launch vehicles, composites offer lighter weight structures that are critical to the mass savings needed to make these vehicles a reality. However NASA is reluctant to use composite laminates because of a lack of experience and confidence in using this material, particularly when the issue of damage tolerance arises. Marshall Space Flight Center Requirement 3479 (MSFC-RQMT-3479) addresses what criteria must be addressed before a composite structure can be used for manned launch vehicles. However, no NASA-built structure has actually gone through the necessary steps involved by this requirements document.

This Technical Publication (TP) describes the development of a material compression design value (not necessarily an allowable) for the material in the acreage area of an interstage structure. This analysis concentrates on the first, and most rigorous, portion of the building block approach—the coupon level testing. Thus a ‘material’ design value (independent of the structure being made) and not a ‘structural’ design value (hardware specific) is being obtained. The structural design value will depend on factors such as scale-up, panel curvature, and processing. The hardware selected and focused on in this study is an interstage structure that is basically a cylindrical sandwich structure that experiences mostly compressive loads. It is expendable and is in flight for only approximately 500 s. This is an ideal type of structure for initial utilization of MSFC-RQMT-3479 because of its simplicity and well-characterized load and temperature profile.

2. MATERIALS

The manufacturing materials for the major part of the composite interstage consist of two equivalent facesheets cocured with an epoxy film adhesive to an aluminum honeycomb core. The epoxy film adhesive used was FM-300K®, a Cytec Industries, Inc. product, with an areal density of 0.08 lb/ft^2. The perforated honeycomb core had a density of 3.1 lb/ft^3 with a 1/8-in cell size. The core was 1.125-in thick, and prior to shipping, was pretreated with a corrosion-resistant coating consisting of a chromate-based protective layer and an organic-metallic polymer.

Two different lay-up schemes were extensively tested as part of this study. These were the base-lined 16-ply quasi-isotropic sandwich structure that had facesheets with an orientation of $[+45,0,-45,90]_{2S}$ and the down-selected 18-ply directional sandwich structure with a lay-up of $[+45,0,-45,0,90,0,0,90,0]_S$. The 16-ply laminates where made of IM7/8552 prepreg material with a 290 g/ft^2 areal weight (0.0115 in/ply nominal) and 66% fiber volume fraction. The 18-ply laminates where made of the same fiber/resin system with a prepreg areal weight of 180 g/ft^2 (0.0064 in/ply nominal) and a 66% fiber volume fraction. The tested specimens were machined from 24- by 24-in panels that were hand laid-up and autoclave cured. The cure cycle was per the manufacturer's recommendation for 8552 epoxy resin. The maximum cure pressure was dropped to 55 psi since processing trials showed this value gives facesheets the best compaction with little draping of the inner plies into the core cells resulting in a laminate with higher compression strength than facesheets cured at 80 or 40 psi.

3. TESTING

The first series of tests directly related to obtaining a material design value for compression after impact (CAI) strength were conducted to find the minimum detectable damage as indicated by flash thermography. This is termed 'damage threshold detection.' Flash thermography was chosen as the measure of damage severity because of its non-invasiveness and ability to assess post-production impact damage at any stage of the structure's life prior to launch. This non-destructive evaluation (NDE) method can detect non-visible damage and by using this parameter, rather than a visual measure, ensures that the structure's weight is best minimized. For the impact testing, the 'worst case' boundary condition for a given impact energy had to be determined.

3.1 Boundary Condition Selection

The boundary condition that gave the most detrimental damage, as detected by flash thermography, for a given impact energy was required as this represents an upper boundary on damage resistance. To assess this, three types of boundary conditions were initially tested with the 16-ply face sheet sandwich specimens. The boundary condition with which the sandwich specimens were supported included simply supported, 'loose,' and 'solid.' For the simply supported boundary condition, the sandwich specimen was supported as a beam with a span of 12 in. This type of boundary condition will be referred to as 'flex.' For the 'loose' boundary condition, the sandwich specimen was resting flat on a metal plate and for the 'solid' impact boundary condition, the sandwich specimen was resting flat on a metal plate with two 10-lb plates on either side of the impact zone to keep the specimen stationary after impact. Schematics of these three boundary conditions are shown in figure 1.

A 0.5-in-diameter tup (impactor) was used for all of the boundary condition impacts. A 4.7-ft lb impact energy was selected as the impact level since this energy is known to give discernable NDE results under a variety of boundary conditions. The results from the boundary condition tests are shown in figure 2.

The data show that the 'loose' and 'solid' boundary conditions gave about the same damage size that was greater than the 'flex' boundary condition. Thus the 'loose' boundary condition (the specimen lying flat on a metal plate with no weights) was chosen for the remainder of this study.

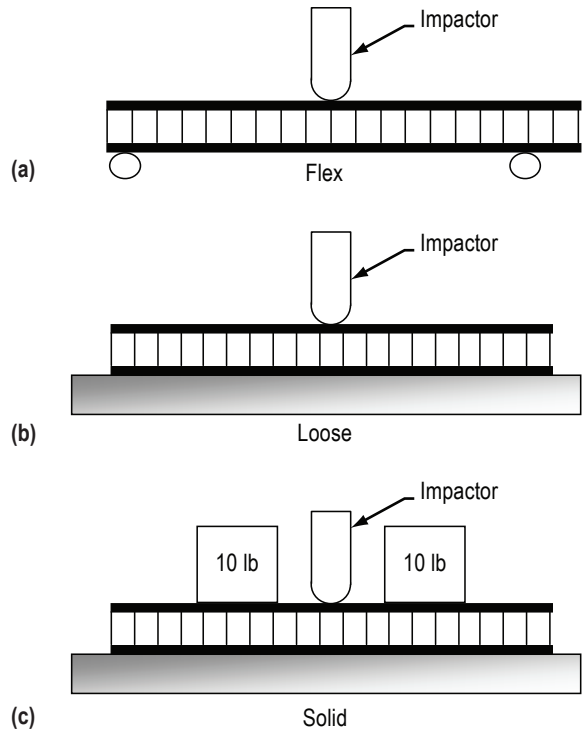

Figure 1. Schematic of the three boundary conditions used in the first series of impacts: (a) flex, (b) loose, and (c) solid.

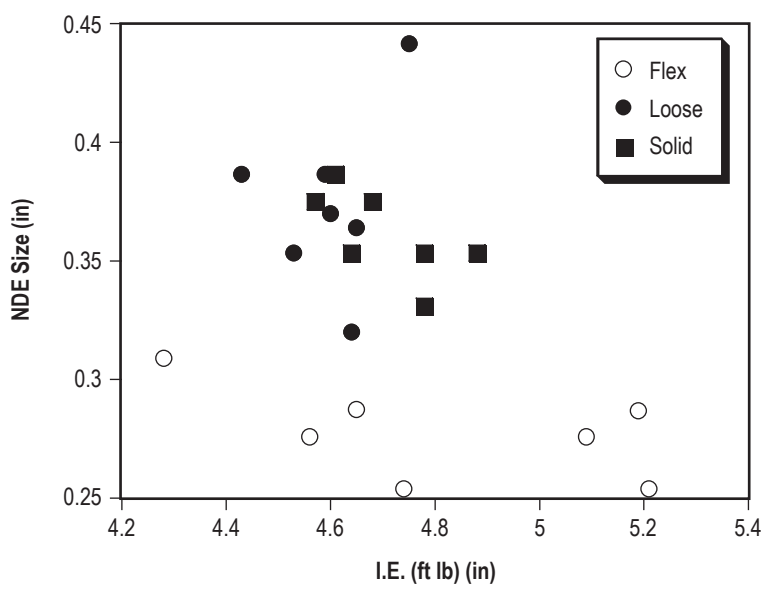

Figure 2. The NDE size versus impact energy results of the boundary condition tests.

3.2 Impact Testing

A drop weight tower was used to impact sandwich specimens with a range of impact energies. A schematic of the apparatus is shown in figure 3. Adjusting the height of the dropped weight varied the impact energy. Three different-sized tups where used in this analysis, 0.25, 0.5, and 1.5 in, to cover a spectrum of possible impacting objects to the composite interstage. The amount of weight used was 2.7 lb for the 0.25- and 0.5-in tups, and 3.7 lb for the 1.5-in tup. The tups were instrumented so that load-time readings could be taken. In addition, the velocity of the falling weight was measured just prior to impact to calculate an impact energy since some of the speed of the falling weight was lost due to friction with the guideposts and the simple weight multiplied by height formula could not be used with accuracy.

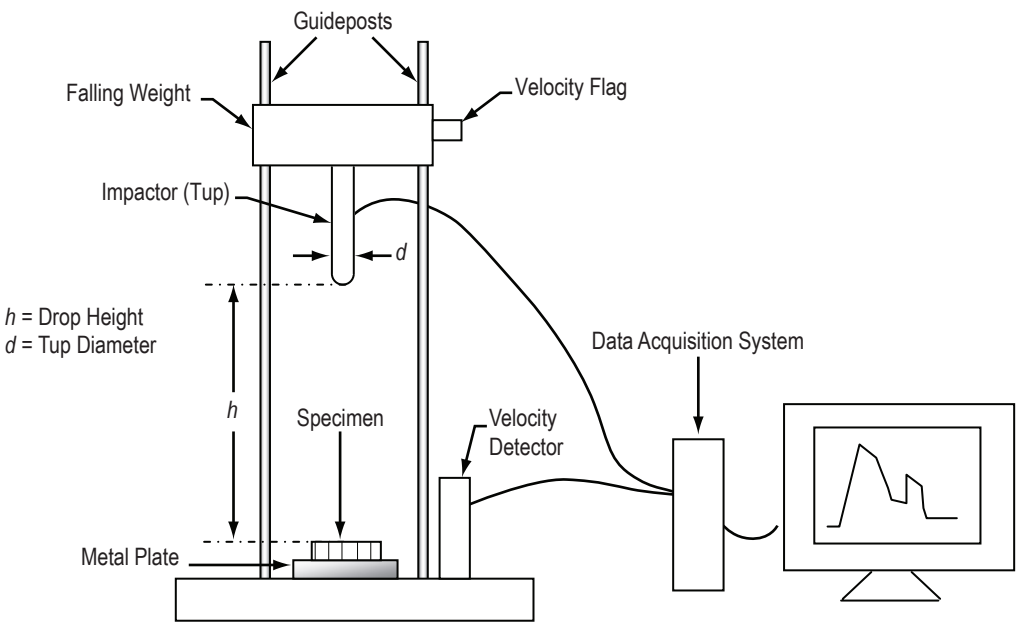

Figure 3. Schematic of impact test apparatus.

3.2.1 Threshold Detection

From the processed 24- by 24-in panels, specimens 12-in-long and 3-in-wide were cut. Each of these specimens was hit at five evenly spaced locations as shown in figure 4. At least three specimens were impacted for a total of 15 impacts minimum for any given tup size.

A range of impact energies was chosen for the series of tests to obtain baseline data for what levels of impact damage the chosen NDE method (flash thermography in this study) could detect.

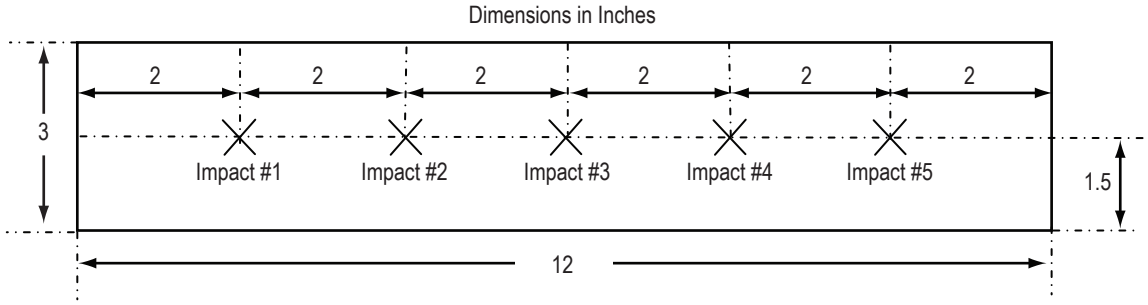

Figure 4. Schematic of impact test specimen with impact locations.

3.2.2 Flash Thermography

Commercial aircraft are subjected to many more impact threats than a one-time-use piece of launch vehicle hardware would be. In addition, an aircraft cannot be inspected with any detail when an impact event does occur since airplanes must be kept flying to be profitable. Thus a simple visual 'look-over' is the measure of damage severity in the commercial transport sector. For the hardware being developed as part of this study, the luxury of minimizing impacts by protecting the hardware, being able to monitor the hardware, and being able to use NDE techniques instead of visual inspection may all be utilized to minimize the structure's weight since this is the ultimate goal of using composite laminates in the first place. The NDE technique chosen to best perform this task was flash thermography.

To perform this type of NDE, the specimen is 'flashed' with a strobe light which heats the specimen's surface. As the surface cools a sensitive infrared (IR) camera is used to monitor the heat loss. Areas with damage will lose heat at a slower rate and the damage can be seen with the IR camera. This technique was chosen because of its non-invasiveness and portability, which make it a likely candidate for inspecting hardware just prior to launch.

The damage, or 'indications,' seen by the camera and data acquisition system are generally circular and the diameter of this circle is termed the damage size as detected by flash thermography.

Flash thermography examples for two 16-ply face sheet specimens hit at 5.0 ft lb are shown in figure 5 for 0.25- and 0.5-in tups.

A flash thermography example for a 16-ply face sheet specimen impacted at 7.5 ft lb is shown in figure 6 for a 1.5-in tup.

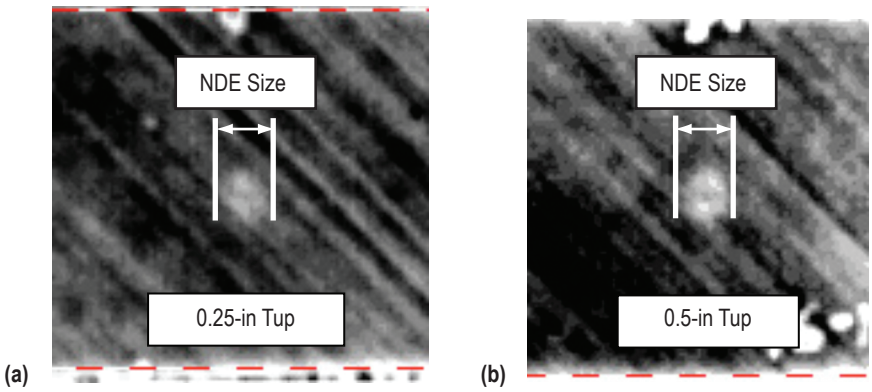

Figure 5. Flash thermography images of two 16-ply face sheet specimens impacted at 5.0 ft lb with (a) 0.25- and (b) 0.5-in tups.

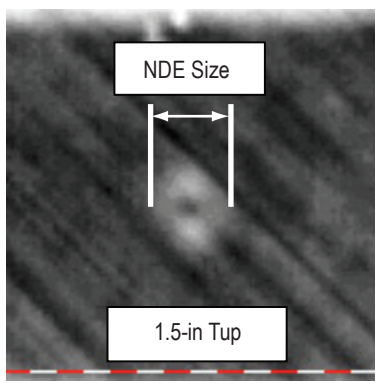

Figure 6. Flash thermography of a 16-ply face sheet specimen impacted at 7.5 ft lb with a 1.5-in tup.

3.2.3 Damaging Compression After Impact Specimens

For the CAI tests the 24- by 24-in sandwich panels were machined into sets of fifteen 4- by 6-in test specimens. Each of these specimens was impacted at the geometric center with a range of impact energies for the three tup sizes used. As data became available, more impacts were performed with the 0.25-in-diameter tup since the smallest tup gave similar CAI results for a given damage size as detected by flash thermography (though not to a great degree), as the 0.5-in- diameter tup. Maximum load of impact, and impact energy were measured for each impacted specimen. Dent depth was also measured for the 18-ply specimens.

3.3 Environmental Effects

Since the composite interstage sees a flight life of ≈500 s, the typical 'hot/wet' testing used by the aircraft industry is much too severe in that overly saturated specimens held at the upper tem-

perature limit for hundreds of hours are tested. This requirement is necessary in aircraft since the environment of the aircraft is not known and the composite parts on these must withstand upper temperature limits for a much longer flight time and a much longer cumulative lifetime. If the intertank does not have thermal insulation applied to it, then the maximum temperature expected on the outer skins is about 220 °F. Preliminary data from beach exposure testing at Cape Canaveral, FL showed that a typical carbon/epoxy laminate gains up to 0.1% moisture depending upon the time of year (the laminates also showed that they could 'dry out' because of a negative moisture level).

The effects of heat and moisture that can be realistically expected for the composite intertank were examined using open hole compression test specimens since they are much more economical to test than those in CAI tests. The specimens consisted of monolithic laminates (no honeycomb) with the 18-ply lay-up. The specimens were end-loaded with the edges being machined to within a ±0.001-in tolerance. A schematic of an open-hole compression test specimen is shown in figure 7.

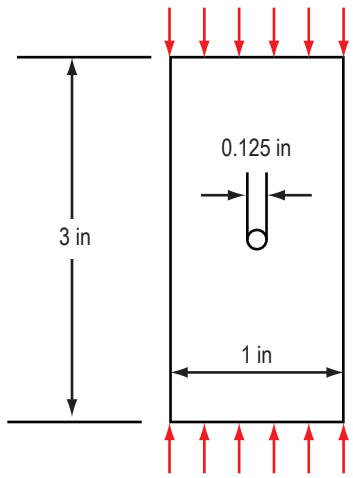

Figure 7. Open hole compression specimens used for environmental effects study.

For the various temperature tests, the specimens were randomly chosen to prevent any bias that might result from taking groups of specimens from the same area of the large panel. Some of the specimens were conditioned in an environmental chamber at 180 °F and 83% relative humidity for about 1 week.

The specimens were conditioned in two batches. The first batch was conditioned to ≈0.7% moisture gain by weight. The second batch was conditioned to ≈0.5% moisture gain by weight. Moisture uptake versus time is shown in figures 8 and 9.

Note that the specimens continued to gain moisture for about 1 day after removal from the environmental chamber. After a day, the specimens slowly lost moisture, but at such a slow rate that the percent moisture uptake right before testing could be known to the nearest 0.1%.

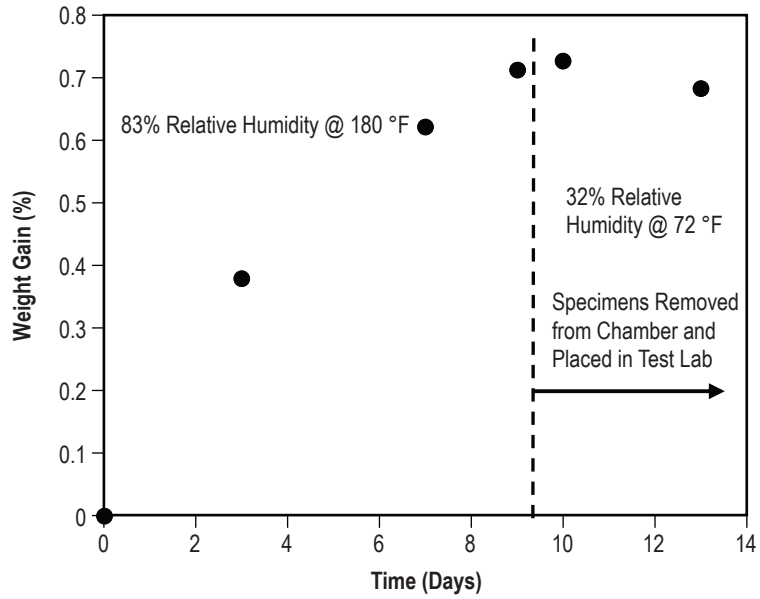

Figure 8. Moisture gain for first batch of specimens.

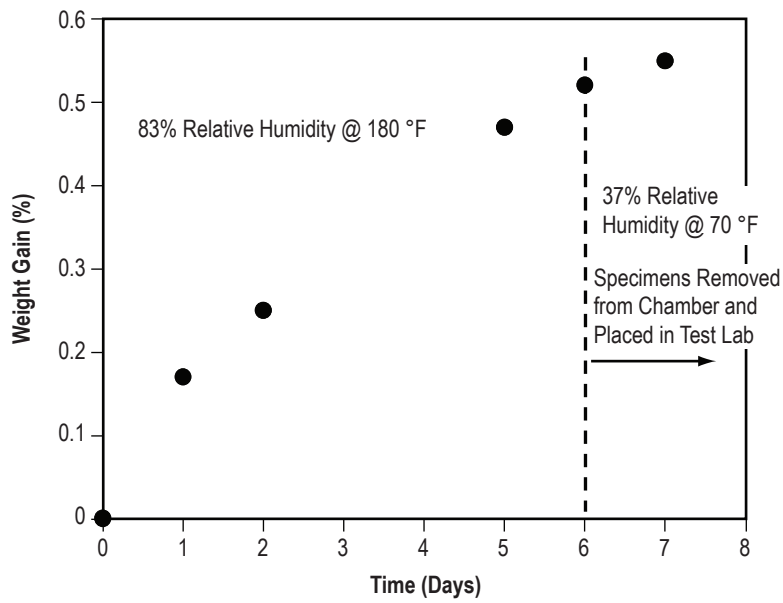

Figure 9. Moisture gain for second batch of specimens.

For open hole compression (OHC) testing, the specimen fixturing was placed in the test chamber and held at temperature for 30 min to allow the steel fixture to come to the designated testing temperature. This was done to prevent biasing the first specimen by creating a heat sink from the specimen to the fixturing. Since there was no trend in any of the data sets, the first specimen tested was always a valid test.

A summary of all of the OHC tests used to evaluate environmental (hot/wet) effects are presented in table 1.

Table 1. Summary of OHC specimens used to evaluate environmental effects.

Test Temperature (°F)	Time @ Temperature (Min)	Moisture Content at Start of Test	No. of Specimens
RT*	–	0.5%	3
RT*	–	None	10
120	10	None	5
150	10	None	3
150	10	0.5%	5
180	10	None	5
180	10	0.5%	3
260	10	None	5
300	10	None	5
300	10	0.7%	5
220	0.17 (10 s)	None	5
220	0.5 (30 s)	None	5
220	3	None	5
220	10	None	5
220	10	0.7%	3
220	30	None	5
220	30	0.7%	5

* RT: Room temperature

3.4 Residual Strength Testing

Once the 4- by 6-in specimens had been impacted, they were prepared for compression testing. This consisted of potting the ends of the specimen into aluminum frames and then precision machining the surfaces so that they were flat and parallel to within a ±0.001-in tolerance. A photograph of a specimen that has been prepared for CAI testing is shown in figure 10 and drawn schematically with dimensions in figure 11. Originally the method in American Society for Testing Materials (ASTM) D7137/7137M was used, however, for specimens that contained little or no damage, specimen buckling, or end brooming tended to occur as shown in figure 12. Thus the 'potted end' technique was subsequently tried and used with success. Once the specimens had been tested and any post mortem examination performed, the aluminum frames could be reused by pyrolyzing the specimen and potting compound out of the frames and then subsequently cleaning any residue on the frames via grit blasting. This allows for reuse of the frames up to five or six times which saves on aluminum material costs. A photograph of a specimen in the load frame used is shown in figure 13.

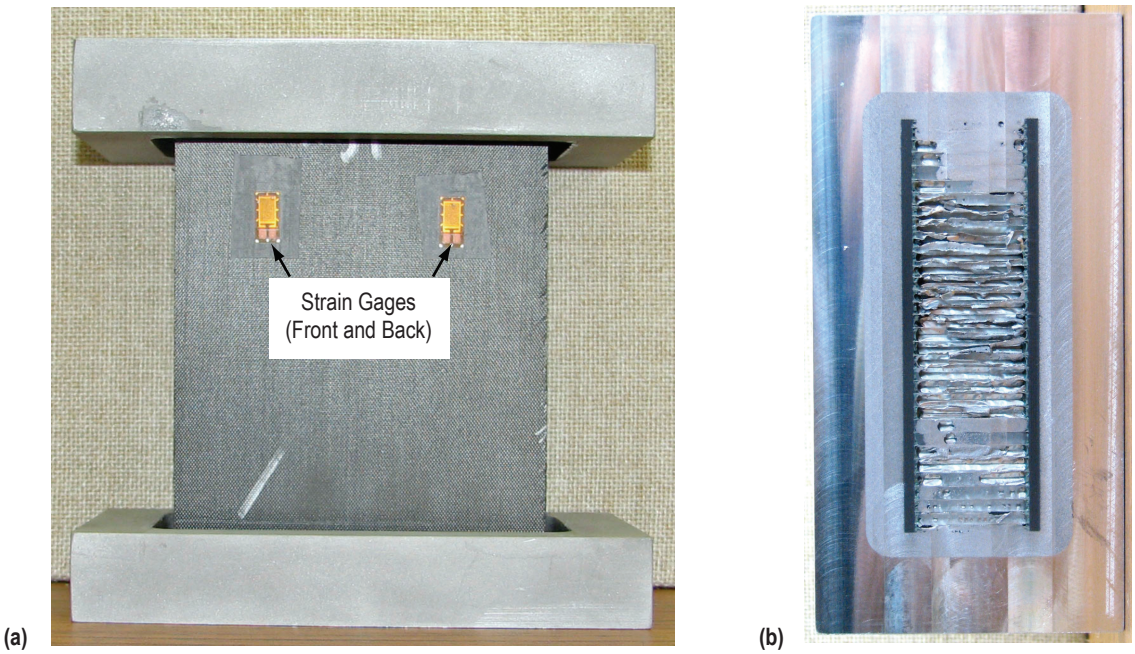

Figure 10. Photograph of a CAI specimen prior to compression testing (a) front view and (b) bottom view.

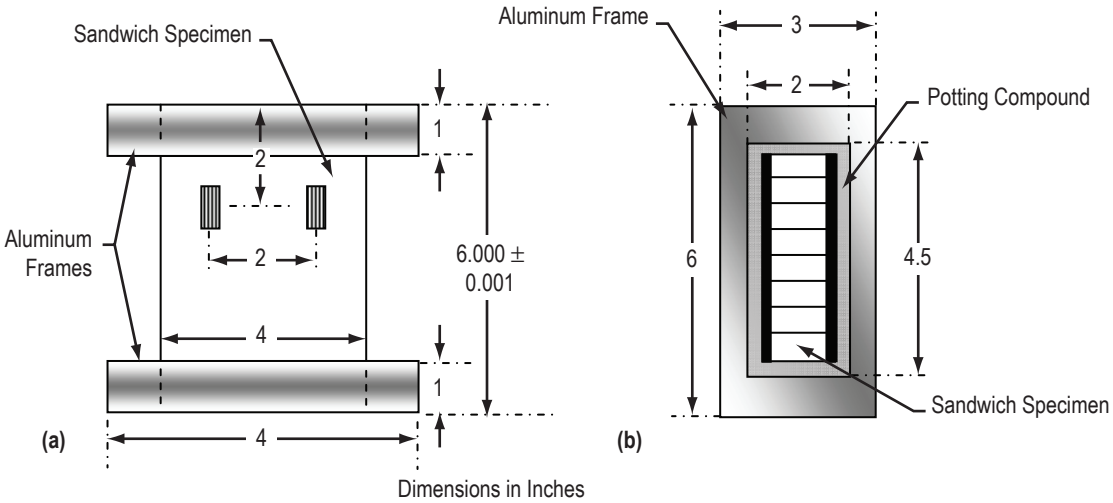

Figure 11. Schematic of a CAI test specimen: (a) front view and (b) bottom view.

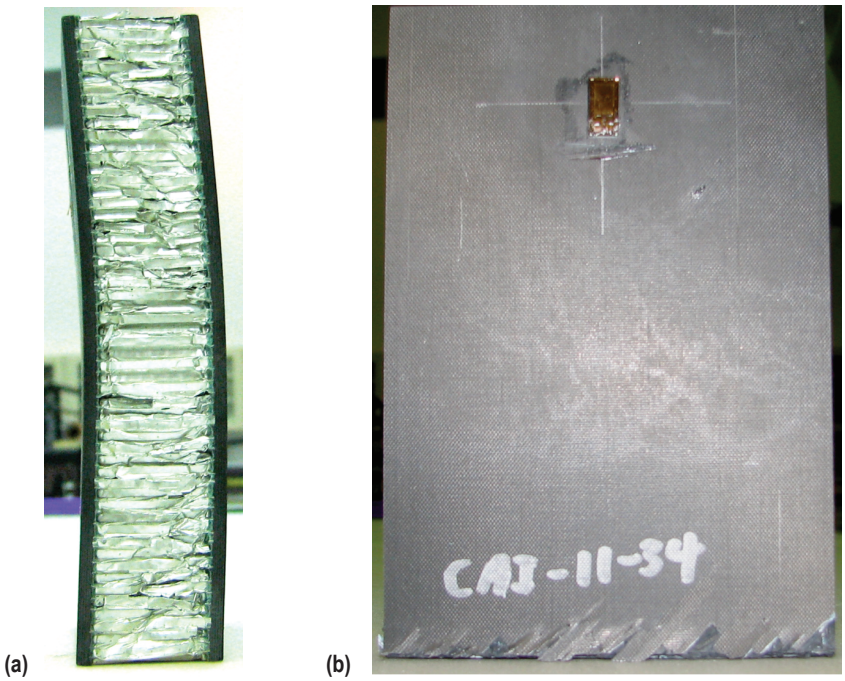

Figure 12. (a) A buckled and (b) end broomed specimen.

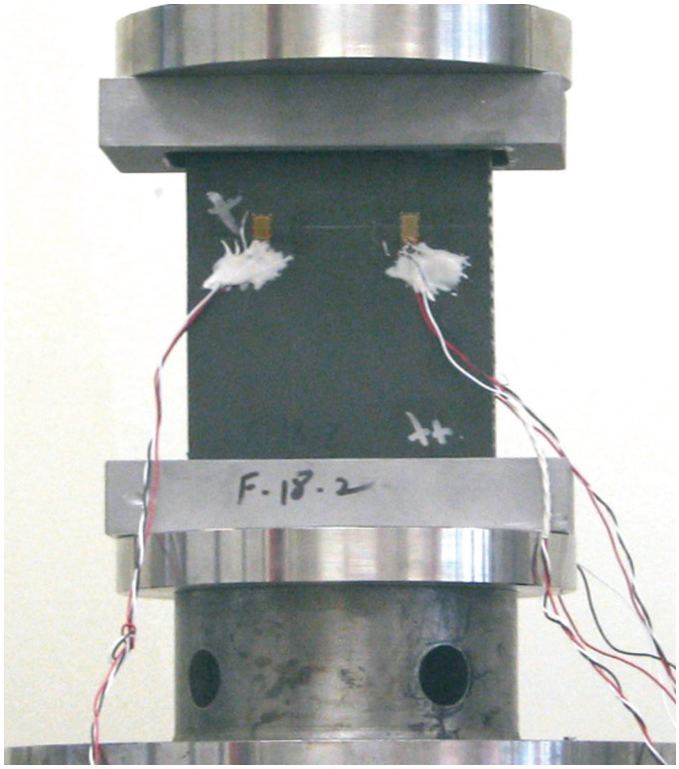

Figure 13. Specimen in a load frame.

In order to ensure that the facesheets were being uniformly loaded, four strain gages were placed on each specimen as shown in figures 10 and 11. During the compression tests, these gages were monitored and if any two of the four deviated more than 10%, the test was stopped and the specimen was appropriately shimmed with 1-mil steel shim stock in order to obtain uniform loading. It was noted that once the specimens were shimmed so that no strain deviation greater than 10% occurred at 5,000 lb, then no additional strain deviation would typically exist upon subsequent loading to failure. It was also noted that all of the deviations were front-to-back, so eventually only two strain gages were used per specimen. If only two gages were applied to a specimen they were placed at the center of the specimen on each side, 2.0 in from the top of the specimen. Typical load versus strain plots are shown in figures 14 and 15.

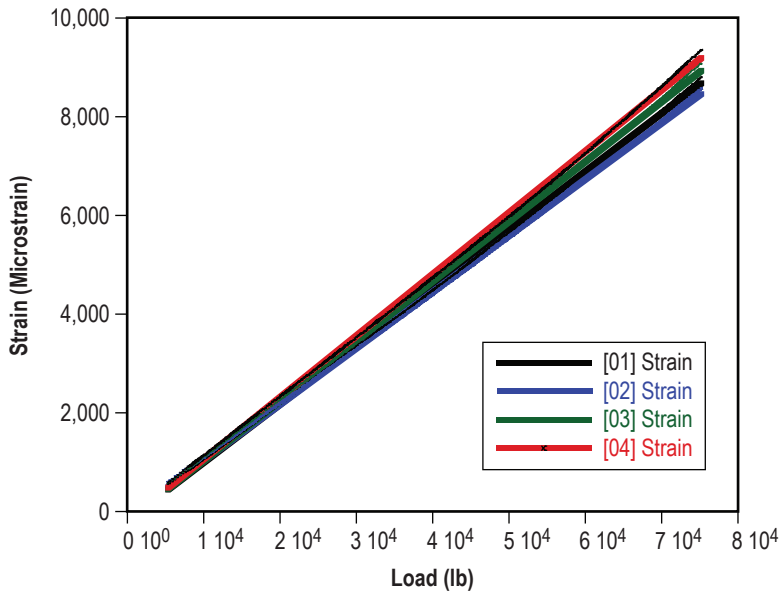

Figure 14. Typical load versus strain plot for 16-ply CAI specimens.

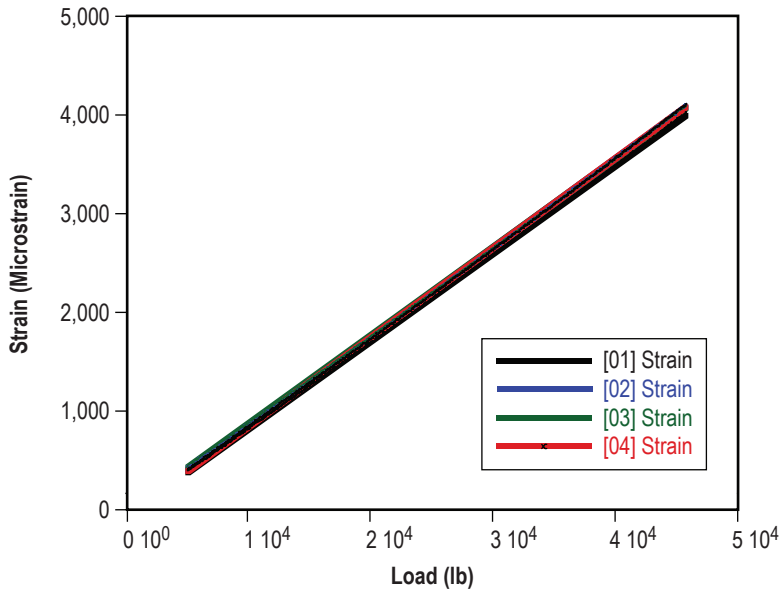

Figure 15. Typical load versus strain plot for 18-ply specimens.

4. RESULTS

4.1 Damage Detection Threshold

The NDE size versus impact energy results are shown in figure 16 for the 16- and 18-ply facesheet specimens impacted with the 0.25-in-diameter tup. The NDE size represents the width of maximum impact damage as detected by flash thermography.

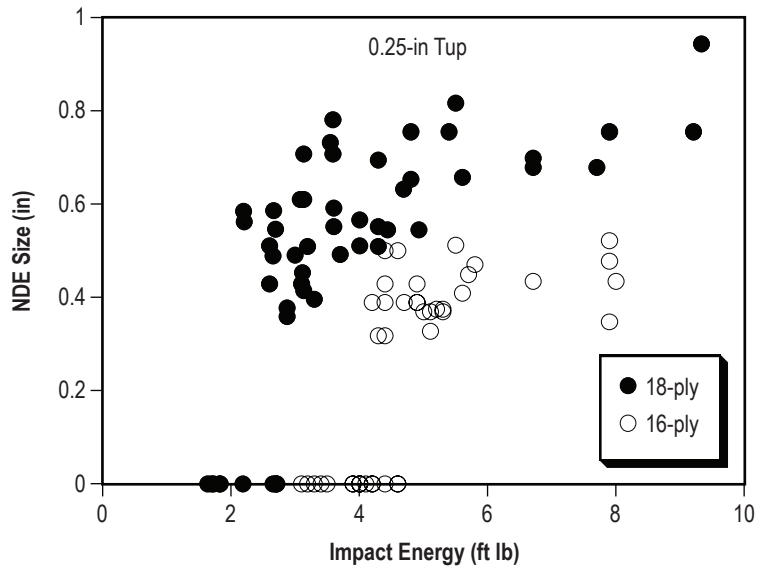

Figure 16. Non-destructive evaluation detection size versus impact energy for 16- and 18-ply facesheet specimens impacted with a 0.25-in tup.

Figure 17 shows the NDE size versus impact energy for the 0.5-in tup. No 18-ply specimens were tested with the 0.5-in-diameter tup.

Figure 18 shows the NDE size versus impact energy for the 1.5-in-diameter tup for the 16- and 18-ply face sheet specimens.

The three plots show that an impact energy of ≈5.0 ft lb or greater will always cause detectable damage for the 0.5- and 0.25-in tup sizes, and an impact energy of ≈7.5 ft lb will always cause detectable damage for the 1.5-in tup. These are the 'threshold,' or barely detectable impact damage (BDID) energies for each tup size. Note however, the 18-ply specimens tended to show detectable damage at lower impact energies than the 16-ply specimens. Thus the BDID threshold for the 18-ply specimens is ≈3 ft lb for both of the tup sizes used (0.25- and 1.5-in-diameter).

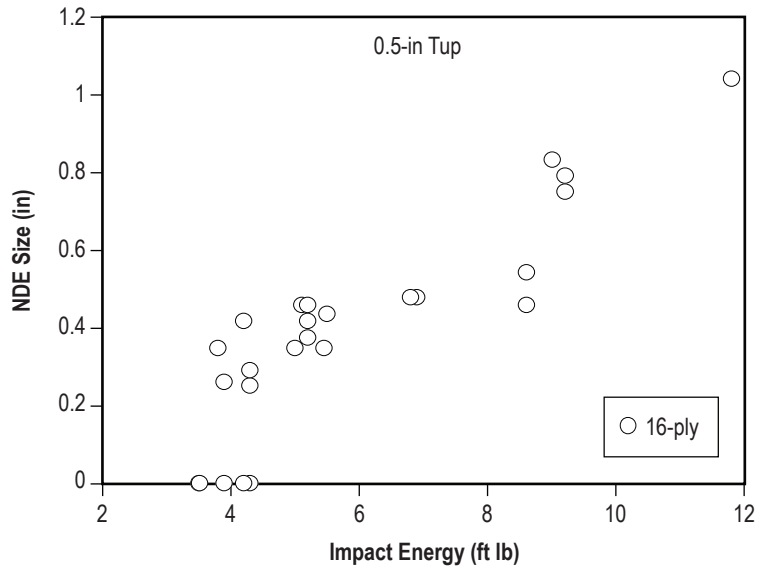

Figure 17. Non-destructive detection size versus impact energy for 16-ply facesheet specimens impacted with a 0.5-in tup.

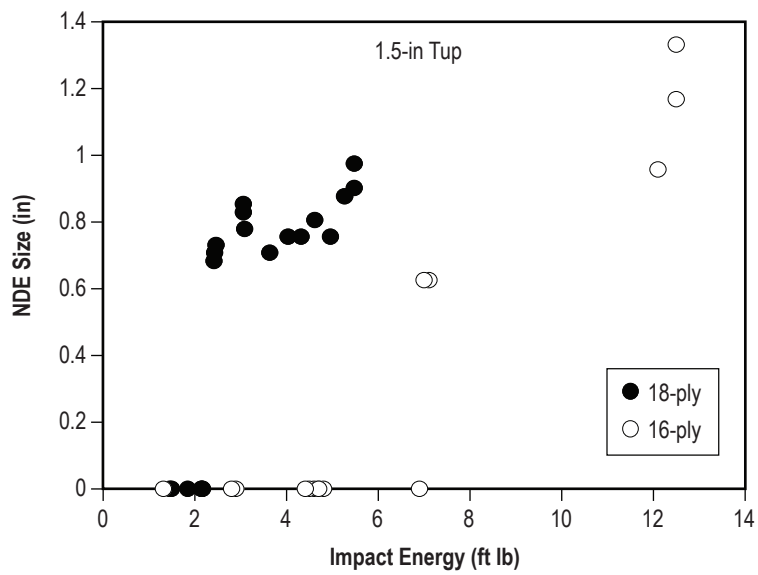

Figure 18. Non-destructive detection size versus impact energy for 16- and 18-ply facesheet specimens impacted with a 1.5-in tup.

It is apparent from the plots in figures 16–18 that there is a discreet jump in measured NDE size for all of the tested specimens. Either no indication was found, or an indication of a discreet size (≈0.3 in for the 0.25- and 0.5-in-diameter tups, ≈0.6 inch for the 1.5-in-diameter tup) was found with no indication of sizes in between. This suggests that there is no damage since damage smaller than

0.6 in would have been seen for the 1.5-in tup-impacted specimens and damage as small as 0.3 in could be detected for the other two tup sizes. In order to better assess these phenomena, specimens that showed no damage via flash thermography at impact energies near the threshold energy were sectioned for microscopy.

Table 2 summarizes the impacts that were microscopically examined for damage. They are all near the damage threshold for a given tup size.

Table 2. Summary of specimens that were cross-sectioned and examined microscopically.

Specimen No.	Impact Energy (ft lb)	Tup Size (in)	NDE Size (in)	Cross-Section
16-15-4	4.6	0.25	0.50	Three minor delaminations with microcracks
16-15-5	4.6	0.25	0	No damage found
16-13-4	4.4	0.25	0.318	Two hairline delaminations with many matrix cracks
16-13-5	4.4	0.25	0	No damage found
16-8-3	4.3	0.5	0.29	Two large delaminations
16-8-4	4.3	0.5	0	No damage found
16-8-5	4.3	0.5	0	Hairline cracks less than one cell width in bottom two plies
16-10-4	7.0	1.5	0.625	Extensive damage
16-10-5	6.9	1.5	0	Very short delamination less than one cell width
18-3	1.7	0.25	0	No damage found
18-6	2.2	0.25	0	No damage found
18-9	2.7	0.25	0	No damage found
18-5	2.2	0.25	0.585	Multiple delaminations
18-13	3.6	0.25	0.780	Multiple delaminations
18-22	3.1	1.5	0.780	Multiple delaminations

Figures 19–23 show select photomicroscopy results.

From the cross-sectional microscopy data, it appears that if flash thermography does not detect any damage, then none of consequence exists. Only a few of the specimens that showed no damage by flash thermography had any detectable damage upon cross-sectional examination. The damage was always less than one cell size if flash thermography did not detect it. The compression tests will help determine if these minor damage states reduce the sandwich structure's compression-carrying ability.

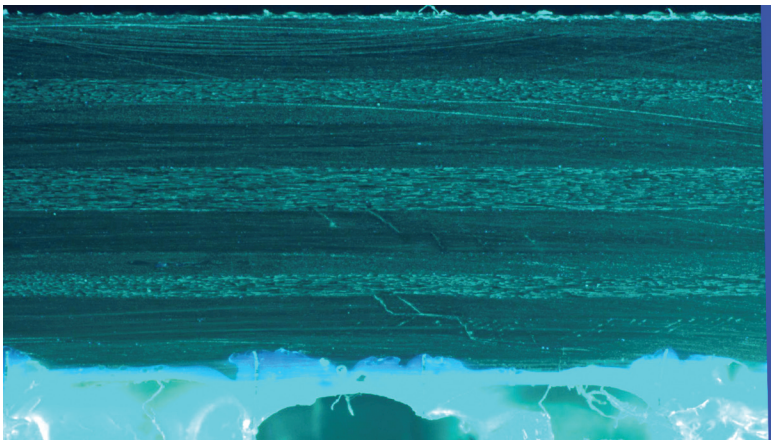

Figure 19. Ultraviolet light enhanced photomicrograph of specimen 16-10-5. No damage detected by flash thermography. Minor delaminations and microcracking about one-half-cell width in size.

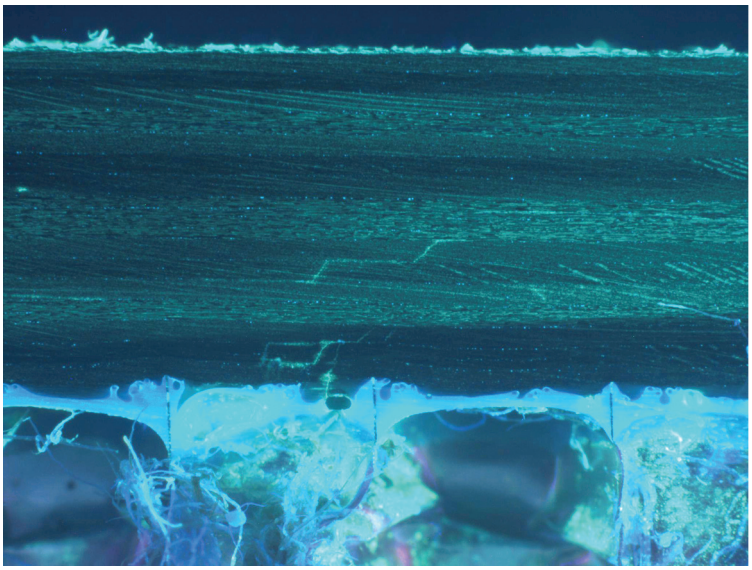

Figure 20. Ultraviolet light enhanced photomicrograph of specimen 16-10-5. No damage detected by flash thermography. Minor damage less than one-cell width seen.

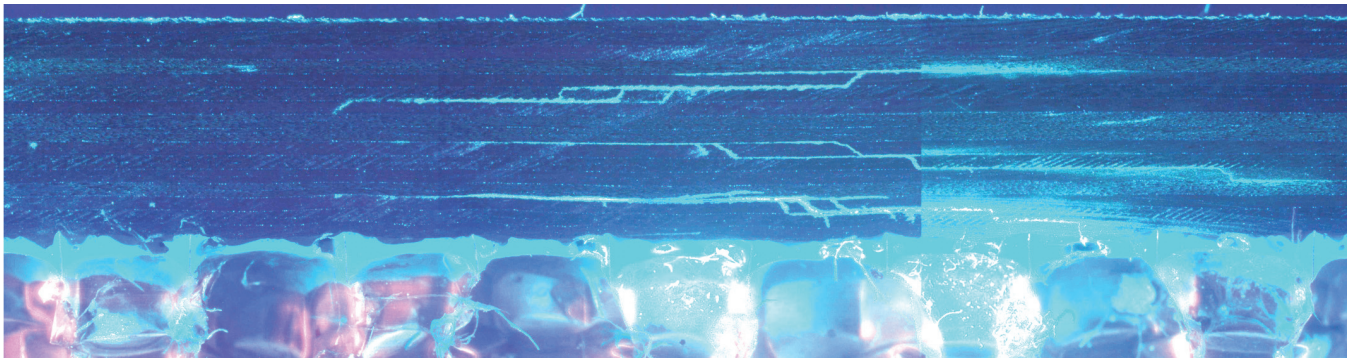

Figure 21. Ultraviolet light enhanced photomicrograph of specimen 16-10-4. Damage size of 0.625 in detected by flash thermography. Delaminations are clearly visible.

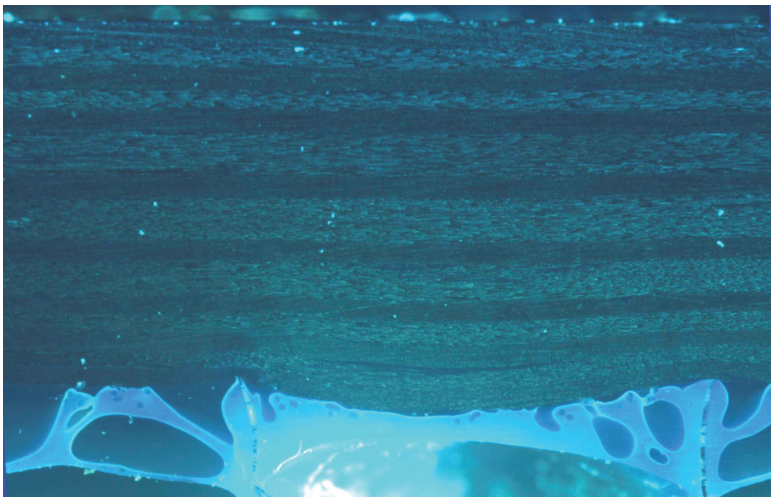

Figure 22. Ultraviolet light enhanced photomicrograph of specimen 18-9. No damage detected by flash thermography. No damage seen upon cross-sectioning.

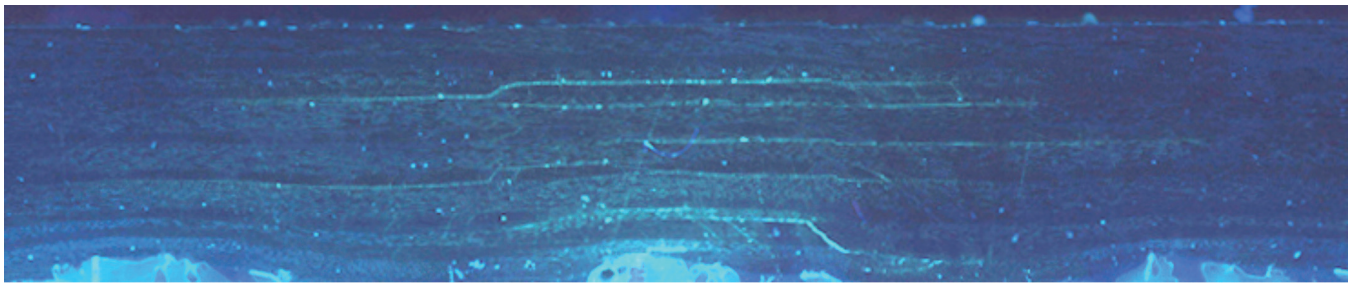

Figure 23. Ultraviolet light enhanced photomicrograph of specimen 18-5. Flash thermography showed an indication size of 0.585.

4.2 Impact of Specimens to be Compression Tested

The specimens to be tested for residual compression strength after impact were 4-in-wide and 6-in-tall. These were impacted with a range of impact energies, but most where impacted near the BDID limit determined in the previous section. These specimens were supported in the same way as were the specimens for the damage detection threshold study. Table 3 summarizes the impacts on the 16-ply CAI samples and table 4 summarizes the impacts on the 18-ply CAI samples. Residual dent depth measurements were taken for the 18-ply specimens since this variable is sometimes used in the aircraft industry as a damage severity indicator.

Table 3. Summary of impacts on the 16-ply CAI samples.

Specimen	Impact Energy (ft-lbs)	Drop Height (in)	Impact Weight (lbs)	Tup Size (in)	NDE 'Size' (in)
CAI-16-1	4.2	20	2.7	0.5	0
CAI-16-2	4.2	20	2.7	0.5	0
CAI-16-3	4.2	20	2.7	0.5	0.42
CAI-16-4	6.3	30	2.7	0.5	0.46
CAI-16-5	6.3	30	2.7	0.5	0.54
CAI-16-6	6.3	30	2.7	0.5	0.46
CAI-16-7	9	46	2.7	0.5	0.83
CAI-16-8	9.2	46	2.7	0.5	0.79
CAI-16-9	9.2	46	2.7	0.5	0.75
CAI-16-10	12.1	44	3.7	1.5	0.96
CAI-16-11	12.5	44	3.7	1.5	1.33
CAI-16-12	12.5	44	3.7	0.5	1.17
CAI-16-13	5.4	26	2.7	0.5	0.46
CAI-16-14	5.4	26	2.7	0.5	0.5
CAI-16-15	14.8	49	3.7	1.5	1.21
CAI-16-16	10.5	50.5	2.7	0.25	0.83
CAI-16-17	10.8	50.5	2.7	0.25	0.83
CAI-16-18	10.9	50.5	2.7	0.5	0.92
CAI-16-19	6.4	30	2.7	0.5	0.54
CAI-16-20	7.4	34.5	2.7	0.5	0.75
CAI-16-21	7.4	37.5	2.7	0.5	0.75
CAI-16-30	3.5	18	2.7	0.25	0
CAI-16-31	4.2	19	2.7	0.25	0.39
CAI-16-32	4.4	20	2.7	0.25	0.43
CAI-16-33	4.7	21	2.7	0.25	0.39
CAI-16-34	4.9	22	2.7	0.25	0.43
CAI-16-35	5.1	23	2.7	0.25	0.37
CAI-16-36	5	24	2.7	0.25	0.37
CAI-16-37	5.6	25	2.7	0.25	0.41
CAI-16-38	5.7	26	2.7	0.25	0.45
CAI-16-39	4	18	2.7	0.25	0
CAI-16-40	4.2	19	2.7	0.25	0
CAI-16-41	4.4	20	2.7	0.25	0.39
CAI-16-42	4.6	21	2.7	0.25	0
CAI-16-43	4.9	22	2.7	0.25	0.39
CAI-16-44	5.1	23	2.7	0.25	0.33
CAI-16-45	5.3	24	2.7	0.25	0.37
CAI-16-46	5.5	25	2.7	0.25	0.51
CAI-16-47	5.8	26	2.7	0.25	0.47
CAI-16-48	4.9	22	2.7	0.25	0.39
CAI-16-49	4	22	2.7	0.25	0.39

Table 4. Summary of impacts on the 18-ply CAI samples.

Specimen	Impact Energy (ft lb)	Drop Height (in)	Impact Weight (lb)	Tup Size (in)	Dent Depth (in)	NDE 'Size' (in)
CAI-18-1	2.6	12	2.7	0.25	0.007	0.428
CAI-18-2	2.6	12	2.7	0.25	0.0055	0.51
CAI-18-3	3.1	14	2.7	0.25	0.006	0.429
CAI-18-4	3	14	2.7	0.25	0.0045	0.49
CAI-18-5	3.6	16.5	2.7	0.25	0.0085	0.551
CAI-18-6	3.6	16.5	2.7	0.25	0.008	0.592
CAI-18-7	4.3	20	2.7	0.25	0.011	0.551
CAI-18-8	4.3	20	2.7	0.25	0.006	0.694
CAI-18-9	4.8	22	2.7	0.25	0.011	0.755
CAI-18-10	4.8	22	3.7	0.25	0.0085	0.653
CAI-18-11	5.5	25	3.7	0.25	0.012	0.816
CAI-18-12	5.4	25	2.7	0.25	0.011	0.755
CAI-18-16	1.8	8	2.7	0.25	0.003	0.83
CAI-18-17	1.8	8	2.7	0.25	0.003	0.83
CAI-18-18	1.8	8	2.7	0.25	0.0035	0.92
CAI-18-19	2.7	12	2.7	0.25	0.0045	0.54
CAI-18-20	2.7	12	2.7	0.25	0.006	0.75
CAI-18-21	2.7	12	2.7	0.25	0.005	0
CAI-18-22	2.7	12	2.7	0.25	0.006	0
CAI-18-23	2.9	13	2.7	0.25	0.0075	0.359
CAI-18-24	2.9	13	2.7	0.25	0.0075	0.377
CAI-18-25	3.1	14	2.7	0.25	0.008	0.415
CAI-18-26	3.1	14	2.7	0.25	0.0085	0.453
CAI-18-27	3.3	15	2.7	0.25	0.009	0.396
CAI-18-28	3.2	15	2.7	0.25	0.0075	0.509
CAI-18-29	3.7	16.5	2.7	0.25	0.010	0.491
CAI-18-30	3.7	16.5	2.7	0.25	0.0095	0.491
CAI-18-31	4	18	2.7	0.25	0.010	0.566
CAI-18-32	4	18	2.7	0.25	0.010	0.510
CAI-18-33	4.3	20	2.7	0.25	0.009	0.509
CAI-18-34	6.7	30	2.7	0.25	0.0145	0.698
CAI-18-35	6.7	30	2.7	0.25	0.0145	0.679
CAI-18-36	7.7	36	2.7	0.25	0.0155	0.679
CAI-18-37	7.9	36	2.7	0.25	0.0175	0.755
CAI-18-38	9.2	42	2.7	0.25	0.0205	0.755
CAI-18-39	9.33	42	2.7	0.25	0.022	0.943
CAI-18-40	4.44	20	2.7	0.25	0.011	0.544
CAI-18-41	4.69	21	2.7	0.25	0.010	0.631
CAI-18-42	4.93	22	2.7	0.25	0.0105	0.544
CAI-18-43	5.6	25	2.7	0.25	0.0125	0.658
CAI-18-44	3.63	12	3.7	1.5	0.0110	0.707
CAI-18-45	4.03	13	3.7	1.5	0.0105	0.756
CAI-18-46	4.31	14	3.7	1.5	0.0120	0.756
CAI-18-47	4.62	15	3.7	1.5	0.0135	0.805
CAI-18-48	4.96	16	3.7	1.5	0.0150	0.756
CAI-18-49	5.26	17	3.7	1.5	0.0130	0.878

4.3 Environmental Effects

The first set of environmental testing was to determine decrease in strength versus dwell time for a given temperature. For this study 220 °F was chosen since analysis has shown this is the highest temperature that the intertank could possibly reach. The specimens were conditioned to 0.7% weight gain, which is much more severe than hardware at Cape Canaveral could experience. The results are plotted in figure 24.

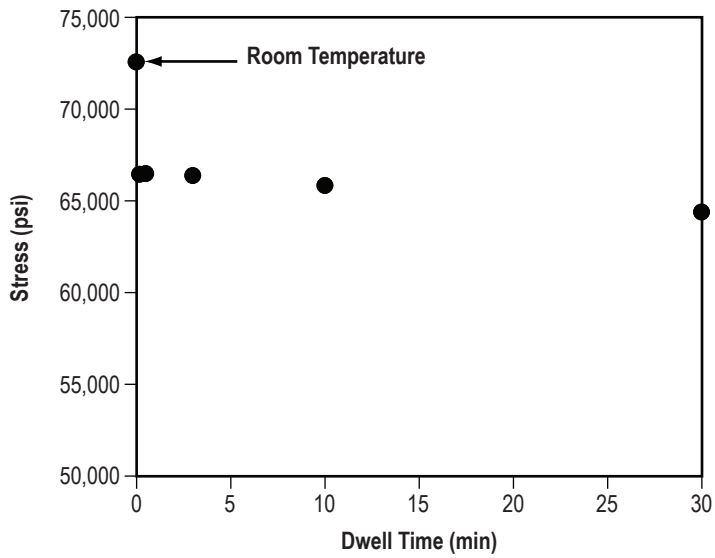

Figure 24. Open hole compression testing results of the various dwell times at 220 °F.

The results show that a small linear decrease in OHC strength is seen as a function of dwell time at 220 °F. This equated to a maximum strength decrease of 3% for the 30-min dwell time. The immediate drop in strength from room temperature (RT) test results is 10%. Thus the total loss of compression strength for a 30-min soak of specimens conditioned to a 0.7% moisture gain at 220 °F amounts to 13%.

For a given dwell time of 10 min (the approximate life of the intertank) the effects of increasing temperature on OHC strength for both conditioned (≈0.5% weight gain for temperatures of 70, 150, and 180 °F; ≈0.7% weight gain for temperatures of 220 and 300 °F), and unconditioned specimens are shown in figure 25.

The effect of moisture tends to decrease the OHC strength when the temperature is elevated, but by only 3% maximum, which is within the scatter of the data.

The OHC strength is reduced with increasing temperature once a temperature of ≈150 °F is reached. At the maximum actual temperature the intertank is expected to reach (220 °F if no thermal insulation is used) the OHC strength drops by about 10%. Designers can use figures 19 and 20 to obtain an estimate of the decrease in compression strength due to temperature. The decrease is small but should be accounted for.

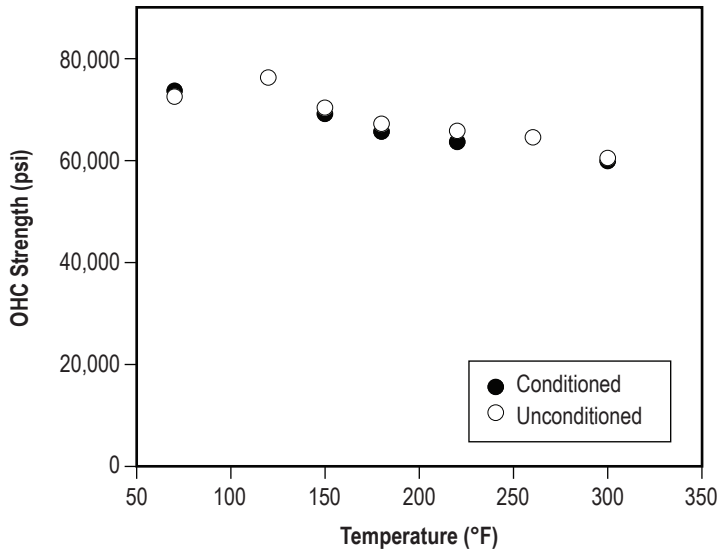

Figure 25. Compression after impact results for various temperatures at a 10-min dwell time.

4.4 Compression After Impact Residual Strength Versus Damage Size

A typical failed 16-ply CAI specimen is shown in figure 26 and a typical failed 18-ply CAI specimen is shown in figure 27.

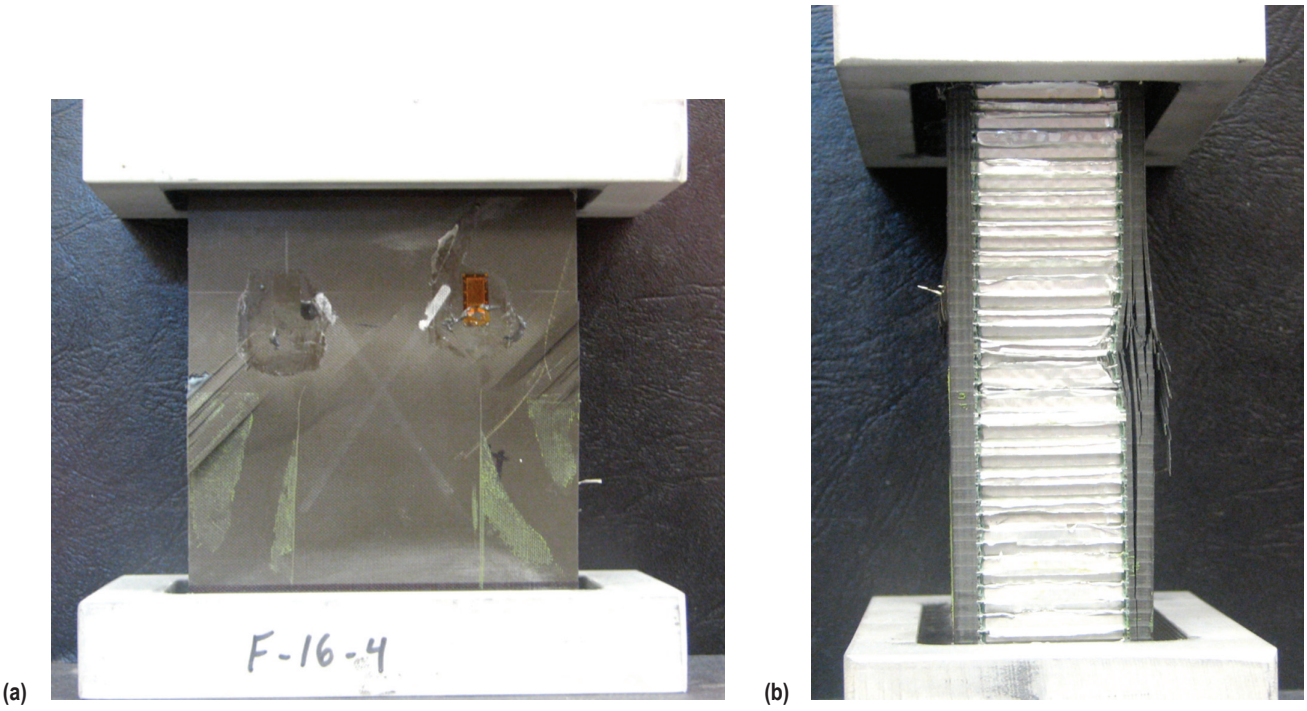

Figure 26. Failed 16-ply compression after impact specimen: (a) front view and (b) side view.

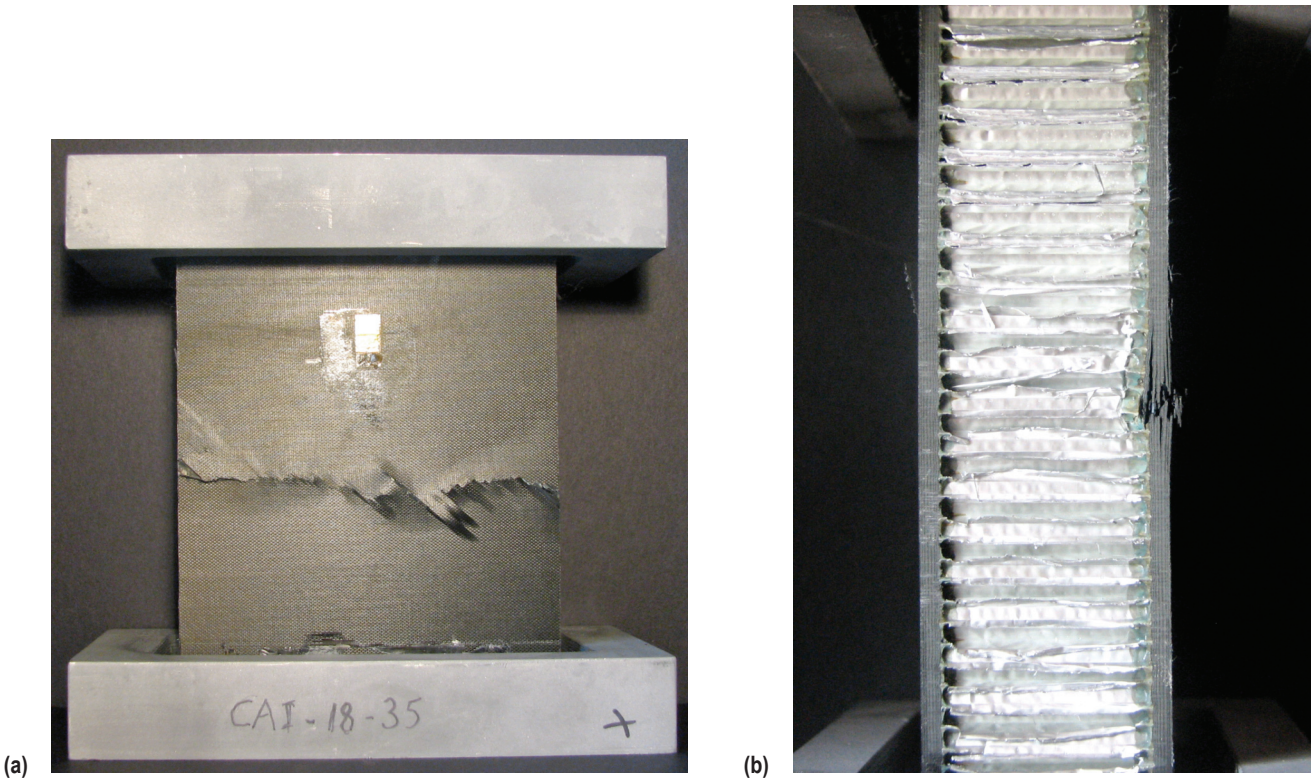

Figure 27. Failed 18-ply compression after impact specimen: (a) front view and (b) side view.

The results from the CAI tests on the 16-ply specimens are plotted in figure 28.

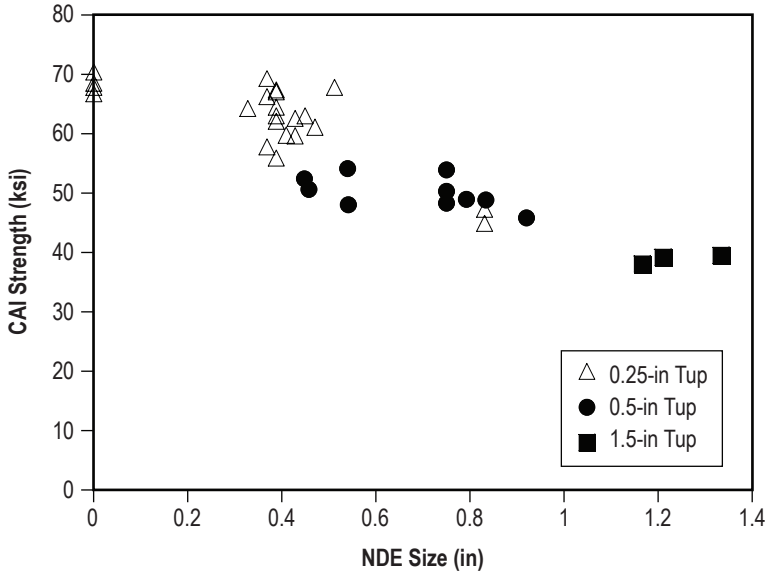

Figure 28. Residual strength versus damage size for all 16-ply impacted specimens.

For the specimens that showed no damage, there was little scatter in the data suggesting that if any existing damage was not detected by NDE, then it was not of consequence.

The tup size appears to have little effect on the CAI values. Pooling the 0.25-, 0.5-, and 1.5-in-diameter tup data and fitting a power curve from where the strength begins to drop gives the curve shown in figure 29. In the equation, $y(x)$ is the predicted CAI strength and x is the damage size in inches.

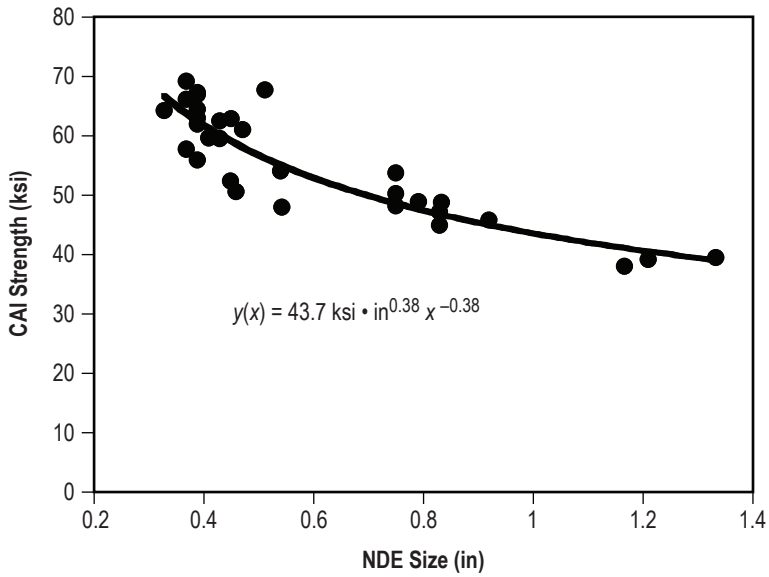

Figure 29. Power curve fit to strength degradation portion of residual strength curve for 16-ply specimens.

The difference between an actual value and predicted value is called a residual. The residual will be positive if the actual value is above the best-fit curve and negative if below the curve. The residuals for the 16-ply specimen data are shown in table 5.

By taking the average value of all of the CAI strength data (55.5 ksi) and adding (or subtracting) the 31 residuals, 31 'normalized' average residual strength values can be obtained based on one damage size and the data can be analyzed with STAT17, an Excel-based statistical analysis program.

Table 5. Residuals from data on the 16-ply specimens.

Specimen	Curve Value (ksi)	Actual Value (ksi)	Residual (R) (ksi)
CAI-16-4	59.3	52.5	–6.8
CAI-16-5	55.1	48.1	–7.0
CAI-16-6	58.8	50.7	–8.1
CAI-16-7	46.8	48.9	+2.1
CAI-16-8	47.7	49.0	+1.3
CAI-16-9	48.7	50.3	+1.6
CAI-16-11	39.1	39.6	+0.5
CAI-16-12	41.2	38.1	–3.1
CAI-16-15	40.6	39.2	–1.4
CAI-16-16	47.3	46.9	–0.4
CAI-16-17	46.9	45	–1.9
CAI-16-18	45.9	45.1	–0.8
CAI-16-19	55.2	54.2	–1.0
CAI-16-20	48.7	48.3	–0.4
CAI-16-21	48.7	53.9	+5.2
CAI-16-31	62.6	64.5	+1.9
CAI-16-32	60.3	62.6	+2.3
CAI-16-33	62.6	56	–6.6
CAI-16-34	60.3	59.7	–0.6
CAI-16-35	63.9	57.9	–6.0
CAI-16-36	63.9	69.3	+5.4
CAI-16-37	61.4	59.8	–1.6
CAI-16-38	59.2	63	+3.8
CAI-16-41	62.6	67.1	+4.5
CAI-16-43	62.6	67.4	+4.8
CAI-16-44	66.8	64.3	–2.5
CAI-16-45	63.9	66.3	+2.4
CAI-16-46	56.4	67.9	+11.5
CAI-16-47	58.2	61.1	+2.9
CAI-16-48	62.6	63.1	+0.5
CAI-16-49	62.6	62.1	–0.5
		Average=55.5	

Putting the 31 'normalized' residual strength values into STAT17 gives an observed level of significance level (OSL) of 0.0224 for a Weibull distribution. This is lower than the required 0.05 so the normal distribution is examined next. The OSL for the normal distribution is 0.258, which is well above the required 0.05, so a normal distribution can be assumed. The B-basis strength value for the normal distribution is 47.9 ksi, (A-basis value of 42.5 ksi). Thus the B-basis strength is 47.9 ksi/55.6 ksi = 0.86 = 86% of the average. Applying this knockdown along the entire best fit power curve gives:

$$y(x)_B=(0.86)y(x) \quad , \tag{1}$$

where

$y(x)_B$ = the B-basis residual strength curve

$y(x)$ = power curve fit given in figure 29.

Figure 30 shows the B-basis residual strength curve plotted with the residual strength data.

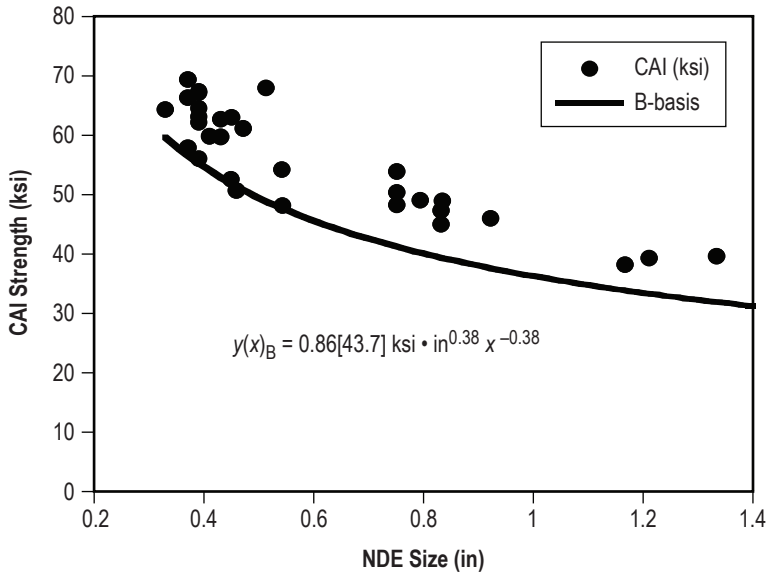

Figure 30. B-basis CAI curve plotted with experimental data for the 16-ply specimens.

The results from the CAI tests on the 18-ply specimens are plotted in figure 31.

For the specimens with no damage size, three of these were unimpacted and showed compression strengths of ≈70 ksi indicating that if no damage was detected by NDE then none of consequence existed.

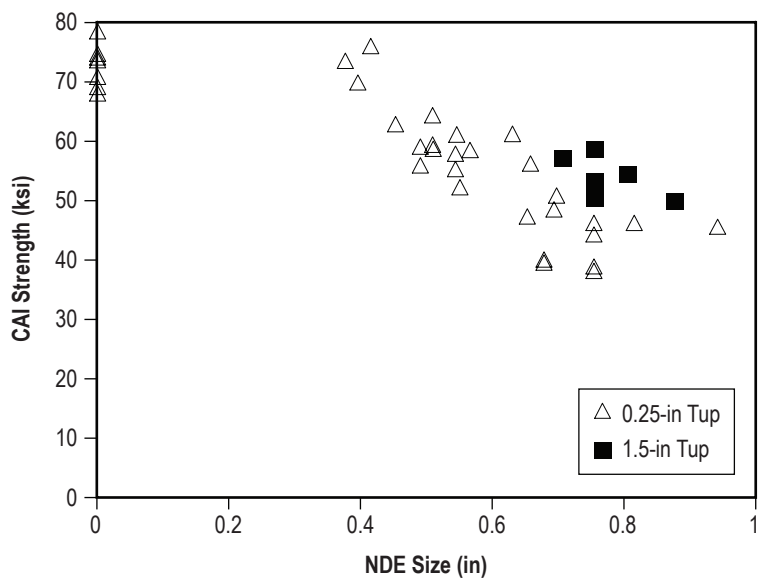

Figure 31. Residual strength versus damage size for all 18-ply impacted specimens.

The tup size does appear to have an effect on the CAI values with the larger tup yielding a higher CAI strength for a given damage size. Separating the 0.25-in-diameter tup data and fitting a power curve from where the strength begins to drop gives the curve shown in figure 32.

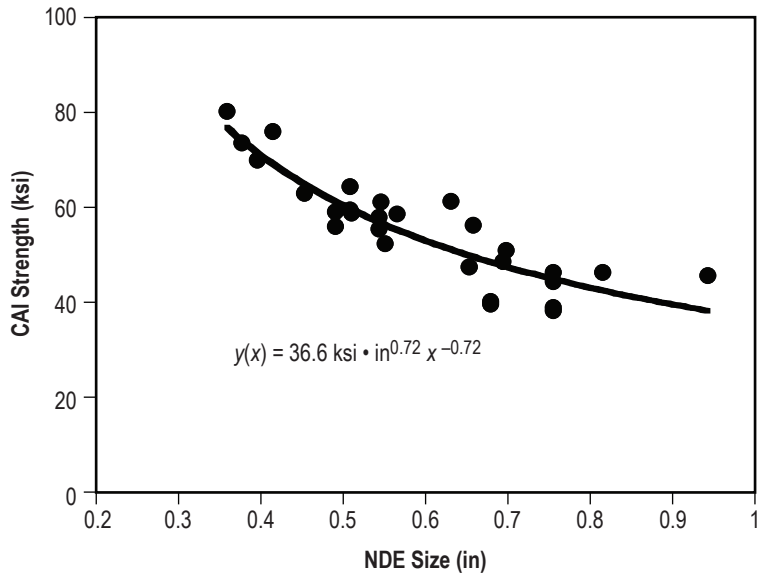

Figure 32. Power curve fit to strength degradation portion of residual strength curve for the 18-ply specimens.

The residuals for the 18-ply specimen data are shown in table 6.

By taking the average value of all of the CAI strength data (55.3 ksi) and adding (or subtracting) the 28 residuals, 28 'normalized' average residual strength values can be obtained based on one damage size and the data can be analyzed with STAT17.

Putting the 28 'normalized' residual strength values into STAT17 gives an OSL of 0.465 for a Weibull distribution. This is larger than the required 0.05 so the Weibull distribution is assumed. From STAT17, the B-basis value for the Weibull distribution is 44.4 ksi, (A-basis of 41.7 ksi). Thus the B-basis strength is 44.4 ksi/55.3 ksi = 0.80 = 80% of the average. Applying this knockdown along the entire best fit power curve gives:

$$y(x)_B=(0.80)y(x) \quad , \tag{2}$$

Figure 33 shows the B-basis curve plotted with the residual strength data.

Table 6. Residuals from data on the 18-ply specimens.

Specimen	Curve Value (ksi)	Actual Value (ksi)	Residual (R) (ksi)
CAI-18-7	56.3	52.3	–4.0
CAI-18-8	47.6	48.5	+0.9
CAI-18-9	44.8	46.2	+1.4
CAI-18-10	49.8	47.3	–2.5
CAI-18-11	42.4	46.2	+3.8
CAI-18-12	44.8	44.3	–0.5
CAI-18-20	56.7	61.1	+4.5
CAI-18-23	76.7	80.1	+3.4
CAI-18-24	74.0	73.5	–0.5
CAI-18-25	69.1	75.9	+6.8
CAI-18-26	64.8	62.8	–2.0
CAI-18-27	71.4	69.8	–1.6
CAI-18-28	59.6	64.3	+4.7
CAI-18-29	61.2	59.0	–2.2
CAI-18-30	61.2	55.9	–5.3
CAI-18-31	55.2	58.5	+3.3
CAI-18-32	59.5	58.7	–0.8
CAI-18-33	59.6	59.4	–0.2
CAI-18-34	47.4	50.9	+3.5
CAI-18-35	48.4	40.1	–8.3
CAI-18-36	48.4	39.6	–8.8
CAI-18-37	44.8	38.2	–6.6
CAI-18-38	44.8	38.9	–5.9
CAI-18-39	38.2	45.6	+7.4
CAI-18-40	56.8	57.9	+1.1
CAI-18-41	51.0	61.2	+10.2
CAI-18-42	56.8	55.3	–1.5
CAI-18-43	49.5	56.2	+6.7
		Average=55.3	

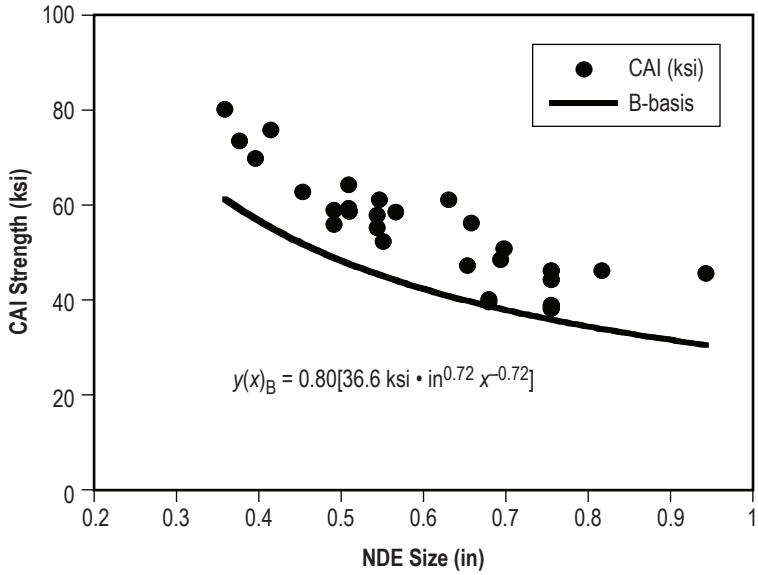

Figure 33. B-basis CAI curve plotted with experimental data for the 18-ply specimens.

4.5 Compression After Impact Versus Dent Depth

If NDE techniques are cost-prohibitive or impractical, then dent depth is sometimes used as a measure of damage severity. Figure 34 shows residual compression strength as a function of dent depth for the 18-ply specimens.

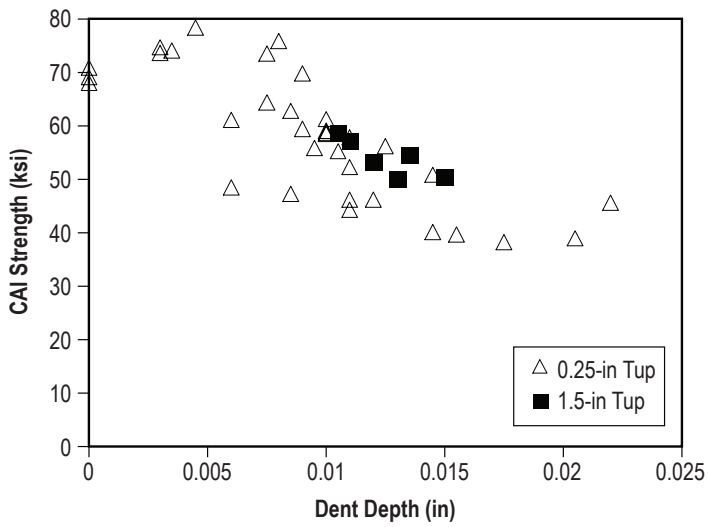

Figure 34. Residual strength versus dent depth for all 18-ply impacted specimens.

The data for the 1.5-in tup appear high, so taking only the 0.25-in tup data and applying a power curve fit gives figure 35.

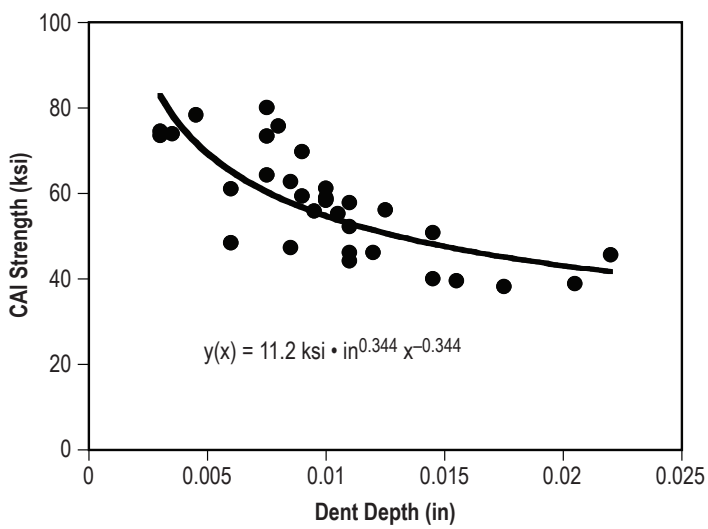

Figure 35. Power curve fit to strength degradation portion of dent depth residual strength curve for the 18-ply specimens.

The residuals for the 18-ply specimen dent depth data are shown in table 7.

Table 7. Residuals from dent depth data on the 18-ply specimens.

Specimen	Curve Value (ksi)	Actual Value (ksi)	Residual (R) (ksi)
CAI-18-7	52.8	52.3	+0.5
CAI-18-8	65.1	48.5	+16.6
CAI-18-9	52.8	46.2	+6.6
CAI-18-10	57.7	47.3	+10.4
CAI-18-11	51.3	46.2	+5.1
CAI-18-12	52.8	44.3	+8.5
CAI-18-16	82.6	74.6	8
CAI-18-17	82.6	73.6	9
CAI-18-18	78.4	74.0	4.4
CAI-18-19	71.9	78.4	–6.5
CAI-18-20	65.1	61.1	+4
CAI-18-23	76.7	80.1	–19.8
CAI-18-24	60.3	73.5	–13.2
CAI-18-25	59	75.9	–16.9
CAI-18-26	57.7	62.8	–5.1
CAI-18-27	56.6	69.8	–13.2
CAI-18-28	60.3	64.3	–4
CAI-18-29	54.6	59.0	–4.4
CAI-18-30	55.6	55.9	–0.3
CAI-18-31	54.6	58.5	–3.9
CAI-18-32	54.6	58.7	–4.1
CAI-18-33	56.6	59.4	–2.8
CAI-18-34	48.1	50.9	–2.8
CAI-18-35	48.1	40.1	8
CAI-18-36	47	39.6	7.4
CAI-18-37	45	38.2	6.8
CAI-18-38	42.7	38.9	3.8
CAI-18-39	41.6	45.6	–4
CAI-18-40	52.8	57.9	–5.1
CAI-18-41	54.6	61.2	–6.6
CAI-18-42	53.7	55.3	–1.6
CAI-18-43	50.6	56.2	–5.6
		Average=57.8	

By taking the average value of all of the CAI strength data (57.8 ksi) and adding (or subtracting) the 32 residuals, 32 ‘normalized’ average residual strength values can be obtained based on one damage size and the data can be analyzed with STAT17.

Putting the 32 ‘normalized’ residual strength values into STAT17 gives an OSL of 0.187 for a Weibull distribution. This is larger than the required 0.05 so the Weibull distribution is assumed. From STAT17, the B-basis value for the Weibull distribution is 41.0 ksi, (A-basis of 27.9 ksi). Thus the B-basis strength is 41.0 ksi/57.8 ksi = 0.71 = 71% of the average. Applying this knockdown along the entire best fit power curve gives:

$$y(x)_B=(0.71)y(x) \quad , \tag{3}$$

Figure 36 shows the B-basis curve plotted with the residual strength data.

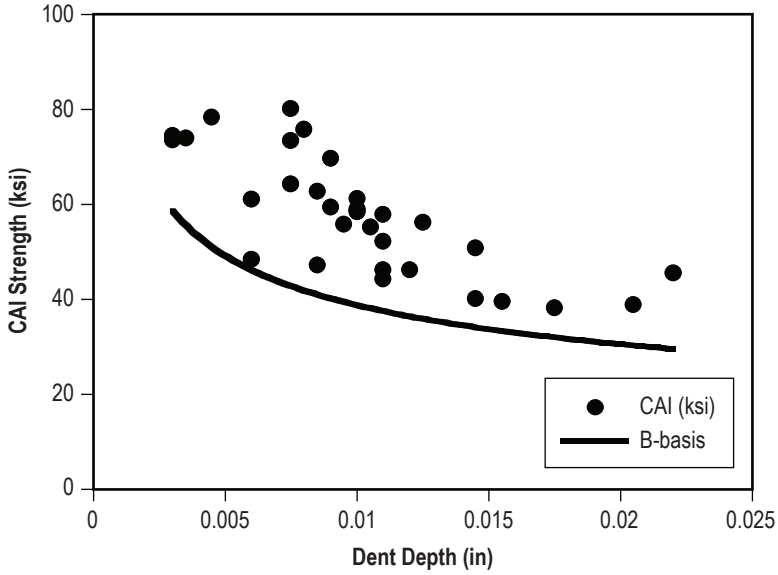

Figure 36. B-basis dent depth versus CAI curve plotted with experimental data for the 18-ply specimens.

Note that the B-basis curve based on dent depth has lower values than the B-basis curve based on damage size. This is due to the higher scatter (residuals) when examining the CAI strength values based on dent depth rather than damage size. Thus if dent depth is the measure of severity of damage as opposed to NDE size as determined by flash thermography, a smaller load for a given damage must be used and the part will have to be designed with less efficiency.

5. CALCULATING A MATERIAL STRENGTH DESIGN VALUE

Once the residual strength curves are defined, a B-basis compression strength with a given size damage can be found for the material of which the intertank acreage is composed. The damage size is limited in this study to a maximum of 1.4 in for the 16-ply lay-up and about 1.0 in for the 18-ply lay-up. Larger damage areas where not tested due to the size limitations of the test specimens, however, only an initial material design value, not a final structural allowable, is being sought.

For 16-ply specimens, the B-basis CAI design value is found by inserting the NDE size into equation (1). For the 18-ply specimens, equation (2) is used. Once this value is found the environmental correction factor (ECF) is applied to the B-basis value. For the data in this study, a conservative value of 0.87 can be applied (from the 220 °F conditioned data). More reasonable estimates can be made once the final maximum temperature, time at temperature, and maximum possible moisture content are better defined.

As an example, suppose the 18-ply laminate is being used as the facesheets for the intertank, and the design limit load is 23.0 ksi, which indicates a preliminary design ultimate load of (1.4)(23 ksi) = 32.2 ksi. Applying the 13% knockdown from the ECF gives a final design ultimate load of 37.0 ksi. From figure 33, replotted as figure 37 with the A-basis residual strength curve, 37.0 ksi corresponds to a B-basis compression strength value associated with a damage size of about 0.75 in as detected by flash thermography. If an A-basis value is used, the maximum damage size allowed is about 0.55 in.

Conversely, for a given damage size, the A- and B-basis ultimate compressive stress can be found from the residual strength curves. Margins of safety can then be calculated to disposition the damage.

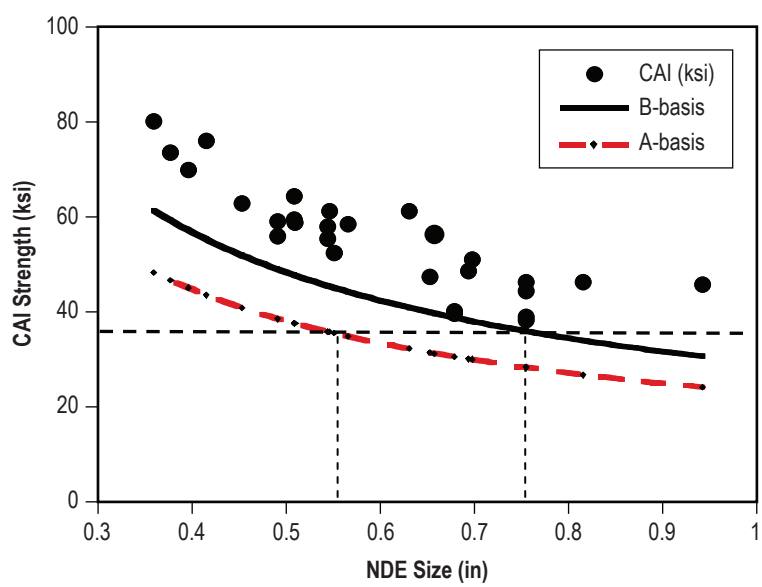

Figure 37. Damage size corresponding to A- and B-basis CAI curve for the 18-ply specimens.

6. CONCLUSIONS

The procedures used to produce a damaged compression material design value for two types of honeycomb sandwich construction have been established. The bulk of the work is in generating the damage severity versus residual strength curves. The next step in the continuation of this work is scaling up to the sub element level. Some of the key observations made in this study are:

- A sandwich structure that has a rigid backing, as opposed to one that is allowed to bend, results in more damage for a given impact energy.

- Unrealistically large moisture uptake for 'wet' specimens can be accomplished in a week.

- End potting of CAI specimens (as opposed to direct edge loading) allowed specimens with little to no damage to be tested without buckling or end brooming.

- A damage threshold exists at which impact damage of a finite size forms. At less severe impacts, there is no damage of significance that forms.

- For specimens with unrealistically high moisture content, the moisture effects of notched compression strength dropped by only 3%.

- Notched compression strength values dropped after ≈150 °F was reached. The strength dropped linearly with increasing temperature. At 220 °F the notched compression strength of 'wet' specimens was reduced by 10%.

- Different size impactors had little effect on CAI strength for quasi-isotropic facesheets, but showed a slightly lower value for small impactors for the directional facesheets.

- A power curve fit, started at the impact severity at which strength drops begin, tends to describe the material compression strength degradation well.

- An A- and B-basis residual strength curve could be determined by 'normalizing' the data at all impact levels to those at the average impact level and applying a percentage knockdown factor to the whole curve.

- Dent depth is not a good indicator of residual compression strength. High knockdowns will result if this is the measure of damage severity. This result has been found in other studies.[1–5]

REFERENCES

1. Tomblin, J.S.; Raju, K.S.; Liew, J.; et al.: "Impact Damage Characterization and Damage Tolerance of Composite Sandwich Airframe Structures,' FAA Report DOT/FAA/AR-00/44, January 2001.

2. Tomblin, J.S.; Raju, K.S.; Acosta, J.F.; et al.: "Impact Damage Characterization and Damage Tolerance of Composite Sandwich Airframe Structures—Phase II,' FAA Report DOT/FAA/AR-02/80, October 2002.

3. Tomblin, J.S.; Raju, K.S.; and Arosteguy, G.: "Damage Resistance and Tolerance of Composite Sandwich Panels—Scaling Effects,' FAA Report DOT/FAA/AR-03-75, February 2004.

4. Tomblin, J.S.; Raju, K.S.; Walker, T.; et al.: "Damage Tolerance of Composite Sandwich Airframe Structures—Additional Results,' FAA Report DOT/FAA/AR-05/33, October 2005.

5. Wardle, B.L.; and Lagace, P.A.: "On the Use of Dent Depth as an Impact Damage Metric for Thin Composite Structures,' *Journal of Reinforced Plastics and Composites*, Vol. 16, No. 12, pp. 1,093-1,110, 1997.

REPORT DOCUMENTATION PAGE

Form Approved
OMB No. 0704-0188

The public reporting burden for this collection of information is estimated to average 1 hour per response, including the time for reviewing instructions, searching existing data sources, gathering and maintaining the data needed, and completing and reviewing the collection of information. Send comments regarding this burden estimate or any other aspect of this collection of information, including suggestions for reducing this burden, to Department of Defense, Washington Headquarters Services, Directorate for Information Operation and Reports (0704-0188), 1215 Jefferson Davis Highway, Suite 1204, Arlington, VA 22202-4302. Respondents should be aware that notwithstanding any other provision of law, no person shall be subject to any penalty for failing to comply with a collection of information if it does not display a currently valid OMB control number.
PLEASE DO NOT RETURN YOUR FORM TO THE ABOVE ADDRESS.

1. REPORT DATE *(DD-MM-YYYY)*
01-01-2009

2. REPORT TYPE
Technical Publication

3. DATES COVERED *(From - To)*

4. TITLE AND SUBTITLE
Developing a Material Strength Design Value Based on Compression After Impact Damage for the Ares I Composite Interstage

5a. CONTRACT NUMBER

5b. GRANT NUMBER

5c. PROGRAM ELEMENT NUMBER

6. AUTHOR(S)
A.T. Nettles and J.R. Jackson

5d. PROJECT NUMBER

5e. TASK NUMBER

5f. WORK UNIT NUMBER

7. PERFORMING ORGANIZATION NAME(S) AND ADDRESS(ES)
George C. Marshall Space Flight Center
Marshall Space Flight Center, AL 35812

8. PERFORMING ORGANIZATION REPORT NUMBER
M–1248

9. SPONSORING/MONITORING AGENCY NAME(S) AND ADDRESS(ES)
National Aeronautics and Space Administration
Washington, DC 20546–0001

10. SPONSORING/MONITOR'S ACRONYM(S)
NASA

11. SPONSORING/MONITORING REPORT NUMBER
NASA/TP—2009–215634

12. DISTRIBUTION/AVAILABILITY STATEMENT
Unclassified-Unlimited
Subject Category 24
Availability: NASA CASI 443–757–5802

13. SUPPLEMENTARY NOTES
Prepared by the Materials and Processes Laboratory, Engineering Directorate

14. ABSTRACT
The derivation of design values for compression after impact strength for two types of honeycomb sandwich structures are presented. The sandwich structures in this study had an aluminum core and composite laminate facesheets of either 16-ply quasi or 18-ply directional lay-ups. The results show that a simple power law curve fit to the data can be used to create A- and B-basis residual strength curves.

15. SUBJECT TERMS
composites, damage tolerance, residual strength

16. SECURITY CLASSIFICATION OF:			17. LIMITATION OF ABSTRACT	18. NUMBER OF PAGES	19a. NAME OF RESPONSIBLE PERSON
a. REPORT	b. ABSTRACT	c. THIS PAGE			STI Help Desk at email: help@sti.nasa.gov
U	U	U	UU	48	19b. TELEPHONE NUMBER *(Include area code)* STI Help Desk at: 443-757-5802

National Aeronautics and
Space Administration
IS20
George C. Marshall Space Flight Center
Marshall Space Flight Center, Alabama
35812